# CHAPTER 5

# COARSE AGGREGATES AND CONCRETES

Normally, coarse aggregate is relatively stronger than other components. Thus, binder is regarded as the weakest link, and consideration about coarse aggregate strength is usually overseen. In concrete mix design, many attempts have been focused on composing aggregate as dense as possible in order to minimize the necessary amount of binder, which has to fill the cavities between the aggregates for a constant workability.

But, when the performance of the binder is improved, leading to increase in concrete strength, the aggregate quality becomes significantly more important. It is desirable that coarse aggregate particles have no defects or weak planes that would cause the aggregate to fail in a brittle manner as the concrete is loaded. The amount of coarse aggregate in concrete mix should be optimized to form an effective load-carrying backbone, and to provide adequate workability in a fresh state for fully compaction.

In this chapter, the coarse aggregates from some selected quarries are investigated experimentally. A parameter, representing both quality and quantity of coarse aggregate, is set up to be an aid in selecting and proportioning coarse aggregate for making high-strength concrete. The appropriate sand/cement ratio is determined regarding to fine aggregate and coarse aggregate compatibility. Consequently, the required amount of binder can be achieved.

## 5.1 Selection of Coarse Aggregate

As stated above, the selection of the coarse aggregate becomes more important as the target compressive strength of concrete increases. The suitable coarse aggregate for producing high-strength concrete must be hard, strong and provide no weak minerals or any defects in its microstructure. A close examination of its mineralogy and petrography may be required to ensure that the aggregate particles are strong enough to avoid premature failure. Nevertheless, many

kinds of crushed hard and dense rocks can be successfully used. Table 5.1 shows the compressive, tensile and shear strength of various types of rock mass. Since the simulations in chapter 2 show that the tensile strength of coarse aggregate for making concrete with compressive strength exceeding 200 MPa should be at least 30 MPa, quartzite, diorite and basalt coarse aggregate may be promising.

The shape of coarse aggregate is also significant from a rheological point of view. During crushing, roughly equi-dimensional particles should be generated, rather than flat and elongated ones. The latter are weak and tend to produce harsh mixes requiring additional water or superplasticizer to achieve the required workability.

It is generally well known that the compressive strength of high-strength concrete will decrease as the coarse aggregate size increases, because the transition zone, as a weak plane, between aggregate particles and binder is reduced. However, some experiences controversially suggested that higher compressive strength can be obtained by using the larger aggregate (Mindess et al, 1996). It is explained that an increase in the total coarse aggregate content, which is more easily attainable with an increase in the maximum size of the aggregate, has the advantage of improving the tensile and fracture properties of concrete, as long as the aggregate is of high quality.

## 5.2 Coarse Aggregate with Various Sizes

### *5.2.1 Size Reduction Process*

Because of their desirable shape and texture, the crushed rocks derived from blasting and crushing are commonly used for making high-strength concrete. The schematic diagram of rock comminution is depicted in Fig. 5.1. After an explosion of rock mass, the boulders are dumped into a hopper, passing grizzly bar and separator. In this step, clay, vegetables or any wastes are removed. Then, serving for primary crushing, a jaw crusher breaks the rocks into smaller pieces. They are crushed further by a cone crusher or impact crusher. This type of crusher easier controls the shape of aggregate, as well as provides more energy than the primary crusher. Next, the crushed rocks are screened and classified according to their size. The particles larger than standard are repeated crushing by the cone crusher until the desired size is obtained, while the particles less then 4.75 mm are considered as dust.

The energy input into the size reduction process must be optimized (Bhandari, 1997). Insufficient energy can not break down the rock, while too much energy provides more dust and induces more microcracks into the microstructure of the aggregate. From the rock mechanics, it is obtained empirically that the energy ( $E$ ) required for size reduction is an inverse function of its size (Nagahama and Yoshii, 1993), i.e.,

$$E = Cr^{-n} \tag{5.1}$$

where $C$ is a constant relating to tensile strength and elastic modulus, while $n$ is a positive number depending on Weibull's coefficient of uniformity of rocks.

Usually, there are weak planes, grain boundaries, voids or any discontinuities in the rock microstructure. Most of the major defects are destroyed from the explosion. Some of the rest are removed in the primary crushing, and little defects are left in the secondary crushing. Thus, it may be deduced that the crushed rock is possibly stronger when its size is reduced.

### *5.2.2 Experimental Works*

The experiment is set up to investigate the characteristics of coarse aggregates with different size. Three types of the mostly-used aggregate in Thailand, i.e., limestone, basalt and granite are evaluated. Limestone aggregates are derived from two quarries in Saraburi province, while two basalt and granite aggregates are come from Burirum and Cholburi province, respectively. All of them are classified regarding to their size into four groups, i.e., 1" (25.40 mm) to 3/4" (19.05 mm), 3/4" (19.05 mm) to 1/2" (12.70 mm), 1/2" (12.70 mm) to 3/8" (9.53 mm) and 3/8" (9.53 mm) to No.4 (4.75 mm). The tested physical properties include specific gravity, water absorption, unit weight, void content, flakiness index and elongation index. While, aggregate crushing value (ACV), aggregate impact value (AIV), Los Angeles abrasion (LAA) and point-load strength index (PLS) represent the mechanical performance. The standard method for each test is tabulated in Table 5.2.

### *5.2.3 Physical Properties*

#### *5.2.3.1 Specific Gravity and Water Absorption*

The plot between the apparent specific gravity and the aggregate size is illustrated in Fig. 5.2. As a characteristic of material, the specific gravity of all types of aggregate is constant. The average values are 2.75, 2.88 and 2.66 for limestone, basalt and granite aggregate, respectively.

While the measured water absorption is depicted in Fig. 5.3. Except for Basalt B, there is a tendency of an increase in water absorption with the size reduction of aggregate. All of them are less than 3.0%. Due to its microstructure, the water absorption of basalt aggregate is higher than limestone and granite aggregate.

#### *5.2.3.2 Unit Weight and Void Content*

Fig. 5.4 shows the relation between unit weight and aggregate size. It reveals that the reduction of aggregate size significantly decreases the value of unit weight. They are about 1610, 1655 and 1554 kg/m$^3$ for 1-inch limestone, basalt and granite aggregate, respectively. They become 1544, 1564 and 1509 when their size is 3/8". While the void content around aggregate particles, as an inverse function of unit weight, increases with decreasing aggregate size. It is shown in Fig. 5.5. For all aggregate size, basalt coarse aggregate provides the most void content compared to the others. It is up to 46.16% for 3/8" basalt A.

#### *5.2.3.3 Flakiness Index and Elongation Index*

The flakiness index of all aggregate samples is shown in Fig. 5.6, while Fig. 5.7 shows the measured elongation index. The flakiness index increases when the aggregate size is reduced. For all aggregate types, the flakiness index of 1-inch aggregate is more or less 10%. It raises up to 45.22%, 72.06% and 53.45% for limestone, basalt and granite aggregate when their size decreases by 3/8". The similar trend is also found in the case of elongation index, except for basalt aggregate where the elongation index is constant for basalt B and decreases with its size for basalt A. In this study, it can be deduced that the comminution process makes the aggregates worse in their shape, leading to go higher amount of void in the granular mixes.

### *5.2.4 Mechanical Properties*

#### *5.2.4.1 Aggregate Crushing Value*

Fig. 5.8 shows the dependence of aggregate crushing value with the aggregate size. It is obvious that aggregate crushing value reduces with the size reduction. It means that the resistance of aggregate for crushing increases when the aggregate size reduces. For 1-inch aggregate, the aggregate crushing values of all types are in the same orders, i.e. 33.18%, 29.13% and 29.22% for limestone, basalt and granite, respectively. They become 21.03%, 12.28% and 18.50% when the size is 3/8". Basalt aggregate is proved to be stronger than granite and limestone aggregate.

### *5.2.4.2 Aggregate Impact Value*

The relation between aggregate impact value and aggregate size is depicted in Fig. 5.9. The similar tendency with size that is found in the case of aggregate crushing value is also revealed here. The average aggregate impact value of 1-inch aggregate is 34.22%, 22.12% and 30.48% for limestone, basalt and granite aggregate, respectively, while those of 3/8" aggregates are 18.97%, 13.30% and 20.01%. It is clear that basalt aggregate provides the most resistance subjected to impact loading.

### *5.2.4.3 Los Angeles Abrasion*

Fig. 5.10 shows the plots between Los Angeles abrasion value and aggregate size. Small increases of Los Angeles abrasion with the reduction of aggregate size can be observed. But, it is not concluded that the resistance of larger aggregate particles are higher then the smaller ones because, according to the standard, the ASTM sieve no.12 is used for screening the remaining from abrasion for all aggregate samples. The probability of smaller aggregates to become particles able to pass the specific sieve is higher than the larger. Thus, in this study, the sieve size depending on sample size that is used for screening the remains for evaluating aggregate crushing value and aggregate impact value, is adopted. The sieve size is tabulated in Table 5.12. This new abrasion value is called the *modified Los Angeles abrasion* (MLAA).

The relation between modified Los Angeles abrasion and aggregate size is shown in Fig. 5.11. Like aggregate crushing value and aggregate impact value, modified Los Angeles abrasion decreases with decreasing aggregate size. The modified Los Angeles abrasion of 1-inch aggregate is 44.67%, 35.49% and 40.91% for limestone, basalt and granite aggregate, respectively. While, those of 3/8-inch aggregates are 35.77%, 27.12% and 32.39%.

### *5.2.4.4 Point-Load Strength Index*

Point-load strength index was introduced by ISRM (1985) as a method for determining the strength of intact rocks with irregular shape. This index correlates to other strength parameters. For example, Broch and Franklin (1972) reported that the uniaxial compressive strength is about 24 times of point load strength index.

In this test, the aggregate size ranges from 10 to 40 mm. The point-load strength index is plotted with aggregate size, as shown in Fig. 5.12. Although the dispersion of test results is

considerable, the trend of point-load strength increasing with size reduction can be observed. The dependence of point-load strength on aggregate size is the largest in limestone aggregate, following by basalt and granite aggregate. However, basalt aggregate yields the highest point-load strength index (13.96 MPa), while that of limestone and granite aggregate are only 10.34 and 7.04 MPa, respectively. This experiment is also confirmed that the comminution process improves the strength of crushed rocks and basalt aggregate is stronger than the others.

## 5.3 Strength-Based Gradation

### *5.3.1 Definition*

When selecting a concrete mix design, it is always desirable to compose coarse aggregate as densely as possible, providing the maximum solid volume. Apart from an obvious economic benefit, a minimum of binder in concrete results in less shrinkage and creep and a more dense, and therefore probably a more durable and strong concrete type. Until now, there have been many attempts to optimize the aggregate gradation. However, in order to make high-strength concrete, such aggregate must also have a superior strength.

The dependence of aggregate performance on aggregate size, which is illustrated in the previous section, makes the selection of aggregate source more complicated. There are many variables for qualifying aggregate quarry, i.e., proportion, shape and strength of each size of crushed rock. Each class of aggregate in an appropriate gradation should possess a good shape and high strength.

Therefore, the idea of *strength-based gradation* (SBG) is presented here as a combination of both physical and mechanical properties in a single concern for determining coarse aggregate gradation. The strength-based gradation index (or SBG Index) is defined as the summation of the products between the fractional volume and strength index of each class of coarse aggregate. For $n$ classes of coarse aggregate, the strength-based packing is

$$\begin{aligned}\text{SBG Index} &= \sum_{i=1}^{n} (\text{fraction volume})_i (\text{strength index})_i \\ &= \sum_{i=1}^{n} (\phi y_i)(S^c)_i \\ &= \phi \sum_{i=1}^{n} y_i S_i^c \end{aligned} \tag{5.2}$$

where $\phi$ is packing density of coarse aggregate mix, which can be computed by using eq. (4.1). $y_i$ and $S_i$ are fractional proportion and strength index of the $i$-th class aggregate, respectively. While, $c$ is the magnifying coefficient corresponding to each type of strength index. The coefficient $c$ is raised due to the fact that the sensitivity of strength index is significantly not in the same degree as that of packing density. It depends on the type of testing for strength index, and will be evaluated from the experiment. Nevertheless, if the strength index of all aggregates equals to one, the SBG index becomes the packing density of the granular mixture. It can be said that the SBG index indicates the potential volume of the strong aggregate particles to provide the concrete strength.

### *5.3.2 Strength Index*

Many parameters have been normally used for representing strength of crushed rock, such as aggregate crushing value, aggregate impact value, Los Angeles abrasion, and point-load strength index. Thus, the strength index ($S_i$) in eq. (5.2) may be derived from one of these parameters, for example, as point-load strength index itself or as the complement to unity of aggregate crushing value, aggregate impact value, Los Angeles abrasion or modified Los Angeles abrasion. That is,

$$
\begin{aligned}
S_{i,PLS} &= PLS \\
S_{i,ACV} &= 1 - ACV \\
S_{i,AIV} &= 1 - AIV \\
S_{i,LAA} &= 1 - LAA \\
S_{i,MLAA} &= 1 - MLAA
\end{aligned}
\tag{5.3}
$$

Because the variation of each strength parameter is different, the magnifying coefficient ($c$) is different for each strength index. To evaluate such coefficients, the concrete specimens are manufactured by varying coarse aggregate. Three types of crushed rock, i.e., limestone A, basalt A, and granite A, are classified regarding to their size and then re-combined to achieve the specified gradation patterns. The gradation patterns of coarse aggregate are shown in Table 5.15. All of them conform to the recommendation of ASTM C33. The maximum size of aggregate is varied in the first four patterns, while, in the last four patterns, all sizes of aggregate are included with a dominated size. The amount of the dominated coarse aggregate is double that of the others.

Portland cement type I is used with the water/cement ratio of 0.20 and 0.24, while the ordinary river sand with fineness modulus of 3.04 is applied with sand/aggregate ratio of 0.45. The ratio of paste volume to void content of compacted aggregate mixture ($\gamma$) is kept constant about 1.10. The mix proportion is shown in Table 5.16. The designation C20-LGP1 means the concrete produced with water/cement ratio of 0.20 and limestone coarse aggregate with gradation pattern no.1. The polymer-based superplasticizer applied to guarantee 110% ±10% of flow value lies between 2% and 3%. After demolding after 24 hours, the concrete specimens are stored under water until the time of testing, i.e., 7, 28, 56 and 91 days for compressive strength.

The measured compressive strength of concrete is tabulated in Table 5.17. At 28 days, they vary from 70.98 MPa to 94.00 MPa in concrete with water/cement ratio of 0.20, and 60.19 MPa to 82.49 MPa in concrete with water/cement ratio of 0.24. It can be observed that, for all types of aggregate and ages of concrete specimens, the measured concrete strength increases when the maximum aggregate size is reduced.

If the concrete compressive strength is expected to be a linear function of SBG indices, the following expression can be obtained, i.e.,

$$f_c' = \mathrm{A}[\text{SBG index}] + \mathrm{B} \tag{5.4}$$

where A and B are arbitrary constants. When the eq. (5.2) is applied, eq. (5.4) becomes

$$f_c' = \mathrm{A}[\phi \sum_{i=1}^{n} y_i S_i^c] + \mathrm{B} \tag{5.5}$$

By using nonlinear regression analysis of the experimental results with the least square basis, the constant A, B and the coefficient $c$ can be evaluated. The magnifying coefficient computing from each type of strength index is tabulated in Table 5.18. The coefficient $c$ corresponding to $S_{i,PLS}$ is only 0.18, while the rest lies more or less 2.0. It is because the aggregate crushing value, aggregate impact value and modified Los Angeles abrasion are in between 0.0 and 1.0, but the point-load strength index is much larger than one. With these magnifying coefficients, the SBG indices of coarse aggregate for each gradation pattern can be calculated. They are listed in Table 5.19, together with packing density computed from eq. (4.1). Opposite to SBG index, the packing density tends to decrease with decreasing maximum size of aggregate. The linear relation between SBG index of coarse aggregate and ratio of concrete to mortar strength is shown in Fig. 5.13. It can be seen that the correlation between concrete to

mortar strength and SBG index computed from the modified Los Angeles abrasion is the best, following by aggregate impact value, aggregate crushing value and point-load strength index. This chart shows the possibility of SBG index to be a potential indicator for concrete strength.

## 5.4 Sand/Aggregate Ratio

The physical interaction between fine aggregate and coarse aggregate is also significant in the performance of concrete. It governs the required amount of binder or cement paste to coat around aggregate particles and fill up the space between them. Sand/aggregate ratio is usually used as a key parameter. The optimum sand/aggregate ratio is required for making high-strength concrete. The ratio of sand to aggregate approximately 0.45 was reported as the best proportion for concrete with 28-day compressive strength up to 100 MPa, regarding both flowability in fresh state and compressive strength in hardened state (Tanpao, 1995, and Leevanichakit, 1995).

With the concept of packing density, which is described in the part 4.1.1, the most favorable sand/cement ratio is both computationally and experimentally determined in this section. Five fine aggregates conforming ASTM C33 are employed. Their fineness modulus is 2.15, 2.45, 2.74, 3.04 and 3.33. While eight gradation patterns for each type of coarse aggregates in the previous section are also applied here. The packing density of each size of aggregate is summarized in Table 5.20.

The packing density of aggregate mixture can be computed by using eq. (4.1). Fig. 5.14 shows the calculated packing density with the mixture composed of fine aggregate with fineness modulus of 3.04 and limestone coarse aggregate with various gradation patterns. It can be seen that the packing density of the mixture decreases when the small particles of coarse aggregate are participated, while the optimum sand/aggregate ratio increases. As shown in Fig. 5.15, when the fineness modulus of fine aggregate decreases, the optimum sand/aggregate ratio decreases, but the maximum packing density of mixture improves. The maximum computed packing density and optimum sand/aggregate ratio of all aggregate proportions are tabulated in Table 5.21. The optimum sand/aggregate ratio varies from 0.37 to 0.64 for the mixtures with limestone coarse aggregate. They become 0.41-0.68 and 0.37-0.60 for those with basalt and granite coarse aggregate, respectively. While the maximum packing density is in between 69.93% and 74.47% for mixtures with limestone coarse aggregate, 69.64% and 73.22% for those with basalt coarse aggregate, and 70.36% and 74.41% for those with granite coarse aggregate.

The optimum sand/aggregate ratio and maximum packing density from the experiment are listed in Table 5.22. The comparison between the calculated and experimental sand/aggregate ratio and maximum packing density are depicted respectively in Fig. 5.16 and Fig. 5.17 for all types of aggregate. Although there is some dispersion of the data, the calculated optimum sand/aggregate ratio matches well to that obtained from the experiment. While the maximum packing density from the experiment is a few percent higher than that from the calculation.

From both computation and experiment, it can be concluded here that the optimum sand/aggregate ratio is not constant and depends on the gradation of fine and coarse aggregate. In concrete mix design, the optimum sand/aggregate ratio should be calculated from the total gradation of aggregate in order to achieve the maximum packing density.

## 5.5 Effective Binder Volume

In concrete, the amount of binder or cement paste must be sufficient to fill up the space between aggregate particles. It means that the minimum quantity of binder equals to the void content of aggregate mixture, i.e., one minus packing density. Nevertheless, due to the workability problem, the amount of binder should be larger than such a value. In practice, the ratio of binder volume to void content of dry and compacted aggregate mixture ($\gamma$) is usually in between 1.1 to 1.4. While seven to ten percent top-up of the binder content is recommended for high-strength concrete (Howard and Leatham, 1989). Because the mechanical performance of aggregate is superior to the binder, the overwhelming amount of binder may detrimental to the load-bearing capacity of concrete.

Thus, in this section, the optimum volume of binder or cement paste for providing the most favorable strength in concrete is determined experimentally. Portland cement type I is used with water/cement ratio of 0.20, whereas 3.04-fineness modulus ordinary river sand is employed with sand/cement ratio varied from 1.0 to 2.0. Three types of crushed rocks, i.e., limestone, basalt and granite, are served as coarse aggregate, with the maximum size of 1", 3/4", 1/2" and 3/8". Sand/aggregate ratio is controlled at 0.45. The 110% ±10% of flow value is guaranteed by the application of polymer-based superplasticizer. The mix proportion is tabulated in Table 5.23. As shown in Table 5.24, the $\gamma$ value of concrete mixes varies from 0.86 to 1.56. When the $\gamma$ value is low, the fresh concrete is viscous and requirs more of superplasticizer. The dosage of superplacticizer is up to 7%.

The total porosity of hardened concrete is tabulated in Table 5.25 as well as plotted with the ratio of binder volume to void content of dry and compacted aggregate ($\gamma$) in Fig. 5.18. At 7 days, the total porosity varies from 8.15% to 12.61%. It shifts in time. The average total porosity is 9.46%, 8.77%, 8.23% and 8.03% at 7, 28, 56 and 91 days, respectively. Regardless to aggregate type, the total porosity seems to be a function of the $\gamma$ value. The $\gamma$ value between 1.0 and 1.1 provides the lowest total porosity.

Table 5.26 and Fig. 5.19 shows the compressive strength of hardened concrete. The inverse tendency to the total porosity can be observed. That is, the highest compressive strength takes place when the $\gamma$ value is in between 1.0 and 1.1. It is up to 128.34 MPa, 161.88 MPa, 165.14 MPa and 168.45 MPa at the age of 7, 28, 56 and 91 days, respectively. Fig. 5.20 shows the plot between the ratio of concrete to mortar strength and $\gamma$ value for each SBG index computed from the aggregate crushing value of coarse aggregate. It can be observed that the ratio of concrete to mortar strength increases with an increasing SBG index. The interaction shown in Fig. 5.21 can be extracted from Fig. 5.20 by a statistical program. It can be noticed that the optimum of $\gamma$ value reduces when SBG index increases. This interaction can be used in concrete mix design. Its usage will be addressed further in the next chapter.

*Table 5.1 Typical strength values of various rocks (Farmer, 1983)*

| Rock Type | Rock Strength (MPa) | | |
|---|---|---|---|
| | Compressive | Tensile | Shear |
| Granite | 100 - 250 | 7 - 25 | 14 - 50 |
| Quartzite | 150 - 300 | 10 - 30 | 20 - 60 |
| Diorite | 100 - 350 | 15 - 35 | 25 - 60 |
| Basalt | 100 - 300 | 10 - 30 | 20 - 60 |
| Shale | 5 - 100 | 2 - 10 | 3 - 30 |
| Sandstone | 20 - 170 | 4 - 25 | 8 - 40 |
| Limestone | 30 - 250 | 5 - 25 | 10 - 50 |

*Table 5.2 Standard methods for evaluating properties of coarse aggregates with various sizes*

| Category | Properties | Standard Method |
|---|---|---|
| Physical | Specific gravity and water absorption | ASTM C127 |
| | Unit weight and void content | ASTM C29 |
| | Flakiness index | BS812: 105.1 |
| | Elongation index | BS812: 105.2 |
| Mechanical | Aggregate crushing value | BS812: 110 |
| | Aggregate impact value | BS812: 112 |
| | Los Angeles abrasion | ASTM C131 |
| | Point-load strength index | ISRM, 1985 |

*Table 5.3 Specific gravity of coarse aggregates with various sizes*

| Rock Type | Specific Gravity | | | |
|---|---|---|---|---|
| | 1" (25.40 mm) | 3/4" (19.05 mm) | 1/2" (12.70 mm) | 3/8" (9.53 mm) |
| Limestone A | 2.724 | 2.719 | 2.744 | 2.782 |
| Limestone B | 2.742 | 2.757 | 2.767 | 2.771 |
| Basalt A | 2.907 | 2.904 | 2.886 | 2.892 |
| Basalt B | 2.887 | 2.878 | 2.859 | 2.848 |
| Granite A | 2.659 | 2.645 | 2.650 | 2.656 |
| Granite B | 2.687 | 2.676 | 2.665 | 2.668 |

*Table 5.4 Water absorption of coarse aggregates with various sizes*

| Rock Type | Water Absorption (%) | | | |
|---|---|---|---|---|
| | 1" (25.40 mm) | 3/4" (19.05 mm) | 1/2" (12.70 mm) | 3/8" (9.53 mm) |
| Limestone A | 0.329 | 0.337 | 0.998 | 1.513 |
| Limestone B | 0.613 | 0.883 | 1.075 | 1.233 |
| Basalt A | 1.417 | 1.431 | 1.886 | 2.645 |
| Basalt B | 1.178 | 1.130 | 1.048 | 1.152 |
| Granite A | 0.569 | 0.682 | 0.797 | 0.851 |
| Granite B | 0.661 | 0.691 | 0.740 | 0.819 |

*Table 5.5 Unit weight of coarse aggregates with various sizes*

| Rock Type | Unit Weight ($kg/m^3$) | | | |
|---|---|---|---|---|
| | 1" (25.40 mm) | 3/4" (19.05 mm) | 1/2" (12.70 mm) | 3/8" (9.53 mm) |
| Limestone A | 1608 | 1593 | 1569 | 1524 |
| Limestone B | 1611 | 1604 | 1587 | 1564 |
| Basalt A | 1647 | 1600 | 1563 | 1557 |
| Basalt B | 1663 | 1622 | 1601 | 1571 |
| Granite A | 1547 | 1536 | 1515 | 1488 |
| Granite B | 1560 | 1546 | 1536 | 1530 |

*Table 5.6 Void content of coarse aggregates with various sizes*

| Rock Type | Void Content (%) | | | |
|---|---|---|---|---|
| | 1" (25.40 mm) | 3/4" (19.05 mm) | 1/2" (12.70 mm) | 3/8" (9.53 mm) |
| Limestone A | 40.96 | 41.39 | 42.83 | 45.23 |
| Limestone B | 41.27 | 41.83 | 42.64 | 43.57 |
| Basalt A | 43.36 | 44.91 | 45.84 | 46.16 |
| Basalt B | 42.41 | 43.64 | 43.98 | 44.85 |
| Granite A | 41.82 | 41.94 | 42.83 | 43.97 |
| Granite B | 41.96 | 42.23 | 42.38 | 42.67 |

*Table 5.7 Flakiness index of coarse aggregates with various sizes*

| Rock Type | Flakiness Index (%) | | | |
|---|---|---|---|---|
| | 1" (25.40 mm) | 3/4" (19.05 mm) | 1/2" (12.70 mm) | 3/8" (9.53 mm) |
| Limestone A | 11.71 | 13.23 | 25.99 | 32.01 |
| Limestone B | 10.52 | 17.29 | 28.72 | 45.22 |
| Basalt A | 7.78 | 8.58 | 35.93 | 72.06 |
| Basalt B | 9.78 | 17.06 | 30.38 | 54.47 |
| Granite A | 8.43 | 11.82 | 13.84 | 36.90 |
| Granite B | 10.43 | 14.90 | 24.16 | 53.45 |

*Table 5.8 Elongation index of coarse aggregates with various sizes*

| Rock Type | Elongation Index (%) | | | |
|---|---|---|---|---|
| | 1" (25.40 mm) | 3/4" (19.05 mm) | 1/2" (12.70 mm) | 3/8" (9.53 mm) |
| Limestone A | 1.21 | 19.29 | 28.91 | 32.10 |
| Limestone B | 4.82 | 21.08 | 34.76 | 41.97 |
| Basalt A | 12.58 | 18.12 | 2.84 | 2.46 |
| Basalt B | 11.36 | 16.73 | 15.19 | 15.95 |
| Granite A | 3.29 | 9.02 | 17.76 | 33.79 |
| Granite B | 6.95 | 16.22 | 26.88 | 28.02 |

*Table 5.9 Aggregate crushing value of coarse aggregates with various sizes*

| Rock Type | Aggregate Crushing Value (%) | | | |
|---|---|---|---|---|
| | 1" (25.40 mm) | 3/4" (19.05 mm) | 1/2" (12.70 mm) | 3/8" (9.53 mm) |
| Limestone A | 32.64 | 29.69 | 25.87 | 19.49 |
| Limestone B | 33.72 | 27.82 | 24.25 | 22.56 |
| Basalt A | 30.26 | 23.11 | 18.54 | 13.97 |
| Basalt B | 28.00 | 23.85 | 17.85 | 10.59 |
| Granite A | 29.37 | 26.47 | 21.33 | 20.36 |
| Granite B | 29.06 | 23.74 | 20.12 | 16.63 |

*Table 5.10 Aggregate impact value of coarse aggregates with various sizes*

| Rock Type | Aggregate Impact Value (%) | | | |
|---|---|---|---|---|
| | 1" (25.40 mm) | 3/4" (19.05 mm) | 1/2" (12.70 mm) | 3/8" (9.53 mm) |
| Limestone A | 33.56 | 29.40 | 22.81 | 18.53 |
| Limestone B | 34.87 | 29.84 | 21.07 | 19.41 |
| Basalt A | 23.87 | 18.35 | 13.38 | 12.16 |
| Basalt B | 20.37 | 17.56 | 14.92 | 14.43 |
| Granite A | 31.55 | 24.56 | 22.15 | 22.58 |
| Granite B | 29.40 | 23.61 | 19.20 | 17.44 |

*Table 5.11 Los Angeles abrasion of coarse aggregates with various sizes*

| Rock Type | Los Angelis Abrasion (%) | | | |
|---|---|---|---|---|
| | 1" (25.40 mm) | 3/4" (19.05 mm) | 1/2" (12.70 mm) | 3/8" (9.53 mm) |
| Limestone A | 23.37 | 24.19 | 26.03 | 30.00 |
| Limestone B | 23.86 | 25.13 | 26.86 | 29.82 |
| Basalt A | 18.72 | 20.02 | 22.42 | 22.90 |
| Basalt B | 19.07 | 19.48 | 19.95 | 20.28 |
| Granite A | 22.75 | 24.05 | 24.94 | 26.60 |
| Granite B | 21.27 | 22.72 | 24.72 | 27.70 |

*Table 5.12 Size of sieves used for screening lost from testing*

| Sample Size (mm) | Sieve Size (mm) | |
|---|---|---|
| | ASTM C131 | BS812: 110 |
| 20.0 - 28.0 | 1.70 | 5.00 |
| 14.0 - 20.0 | 1.70 | 3.35 |
| 10.0 - 14.0 | 1.70 | 2.36 |
| 6.30 - 10.0 | 1.70 | 1.70 |
| 5.00 - 6.30 | 1.70 | 1.18 |
| 3.35 - 5.00 | 1.70 | 0.85 |
| 2.36 - 3.35 | 1.70 | 0.60 |

*Table 5.13 Modified Los Angeles abrasion of coarse aggregates with various sizes*

| Rock Type | Modified Los Angelis Abrasion (%) | | | |
|---|---|---|---|---|
| | 1" (25.40 mm) | 3/4" (19.05 mm) | 1/2" (12.70 mm) | 3/8" (9.53 mm) |
| Limestone A | 44.16 | 37.84 | 35.82 | 35.56 |
| Limestone B | 45.17 | 41.40 | 40.30 | 35.97 |
| Basalt A | 35.76 | 30.91 | 29.13 | 28.10 |
| Basalt B | 35.22 | 29.95 | 26.34 | 26.14 |
| Granite A | 39.91 | 35.57 | 33.17 | 30.97 |
| Granite B | 41.90 | 36.03 | 33.11 | 33.80 |

*Table 5.14 Point-load strength index of coarse aggregates with various sizes*

| Limestone A | | Limestone B | | Basalt A | | Basalt B | | Granite A | | Granite B | |
|---|---|---|---|---|---|---|---|---|---|---|---|
| Size (mm) | PLS (MPa) | Size (mm) | PLS (MPa) | Size (mm) | PLS (MPa) | Size (mm) | PLS (MPa) | Size (mm) | PLS (MPa) | Size (mm) | PLS (MPa) |
| 25.2 | 5.77 | 16.0 | 7.00 | 22.3 | 11.16 | 18.7 | 11.00 | 32.5 | 3.89 | 25.1 | 4.65 |
| 32.1 | 6.35 | 33.1 | 5.30 | 16.4 | 13.48 | 15.6 | 12.14 | 28.2 | 3.88 | 28.3 | 4.82 |
| 27.5 | 7.06 | 26.3 | 4.32 | 18.2 | 9.56 | 22.3 | 12.56 | 25.6 | 4.51 | 30.2 | 5.23 |
| 17.8 | 7.92 | 17.6 | 8.06 | 24.6 | 9.59 | 24.6 | 11.98 | 28.2 | 4.85 | 26.1 | 5.47 |
| 15.3 | 10.01 | 21.8 | 7.23 | 26.1 | 12.03 | 31.5 | 10.62 | 16.5 | 4.45 | 18.5 | 5.59 |
| 21.6 | 10.26 | 23.5 | 6.43 | 19.0 | 12.52 | 32.5 | 11.67 | 24.2 | 4.92 | 16.9 | 4.29 |
| 21.3 | 7.49 | 19.3 | 5.24 | 22.5 | 12.39 | 28.6 | 8.54 | 18.3 | 5.69 | 23.4 | 5.18 |
| 30.4 | 8.63 | 29.7 | 6.26 | 30.2 | 12.21 | 24.8 | 9.47 | 22.5 | 5.50 | 32.5 | 5.45 |
| 23.8 | 7.57 | 26.3 | 6.48 | 16.4 | 8.99 | 25.5 | 11.33 | 29.2 | 5.51 | 31.1 | 5.00 |
| 17.6 | 10.07 | 34.0 | 3.63 | 22.7 | 8.14 | 19.3 | 13.96 | 18.9 | 3.61 | 22.4 | 5.54 |
| 19.4 | 6.93 | 18.6 | 7.39 | 32.4 | 11.73 | 21.4 | 13.39 | 20.8 | 4.66 | 21.6 | 4.40 |
| 25.8 | 6.68 | 35.1 | 6.22 | 15.7 | 12.02 | 23.2 | 11.81 | 27.3 | 5.10 | 28.9 | 3.73 |
| 22.0 | 7.12 | 32.2 | 6.32 | 28.8 | 11.26 | 31.0 | 9.21 | 19.6 | 5.11 | 20.6 | 4.73 |
| 35.4 | 6.14 | 24.8 | 5.92 | 28.3 | 7.72 | 27.5 | 11.09 | 23.5 | 3.86 | 27.5 | 5.04 |
| 24.7 | 7.15 | 20.6 | 6.31 | 24.7 | 11.91 | 24.1 | 11.13 | 31.1 | 5.00 | 26.6 | 4.25 |
| 15.3 | 7.51 | 18.2 | 5.74 | 23.8 | 11.35 | 16.5 | 8.90 | 34.6 | 4.94 | 28.2 | 5.82 |
| 24.2 | 8.60 | 13.4 | 6.15 | 26.2 | 13.04 | 19.2 | 12.32 | 18.3 | 5.69 | 35.1 | 4.84 |
| 26.1 | 4.37 | 21.9 | 5.74 | 30.3 | 10.41 | 20.4 | 12.81 | 24.3 | 4.89 | 19.2 | 7.04 |
| 17.3 | 10.34 | 23.6 | 5.11 | 20.7 | 9.40 | 32.5 | 10.12 | 27.6 | 3.01 | 21.3 | 5.99 |
| 20.8 | 9.33 | 28.1 | 2.93 | 19.5 | 13.74 | 18.1 | 9.64 | 30.5 | 4.29 | 25.1 | 3.49 |

*Table 5.15 Gradation patterns for producing concrete with various SBG indices*

| Gradation Pattern | Cumulative Percentage Passing | | | |
|---|---|---|---|---|
| | 1" (25.40 mm) | 3/4" (19.05 mm) | 1/2" (12.70 mm) | 3/8" (9.53 mm) |
| No. 1 | 100 | 75 | 50 | 25 |
| No. 2 | 0 | 100 | 67 | 33 |
| No. 3 | 0 | 0 | 100 | 50 |
| No. 4 | 0 | 0 | 0 | 100 |
| No. 5 | 100 | 60 | 40 | 20 |
| No. 6 | 100 | 80 | 40 | 20 |
| No. 7 | 100 | 80 | 60 | 20 |
| No. 8 | 100 | 80 | 60 | 40 |

*Table 5.16 Mix proportion of concretes with various SBG indices*

| Designation | Cement ($kg/m^3$) | Water ($kg/m^3$) | C. Aggregate ($kg/m^3$) | Sand ($kg/m^3$) | Superplas. ($kg/m^3$) |
|---|---|---|---|---|---|
| C20-LGP1 | 531 | 106 | 1102 | 901 | 11 |
| C20-LGP2 | 543 | 109 | 1092 | 893 | 11 |
| C20-LGP3 | 561 | 112 | 1077 | 881 | 14 |
| C20-LGP4 | 577 | 115 | 1064 | 871 | 14 |
| C20-LGP5 | 525 | 105 | 1106 | 905 | 11 |
| C20-LGP6 | 529 | 106 | 1104 | 903 | 11 |
| C20-LGP7 | 535 | 107 | 1098 | 899 | 11 |
| C20-LGP8 | 538 | 108 | 1096 | 897 | 11 |
| C24-LGP1 | 493 | 118 | 1102 | 901 | 10 |
| C24-LGP2 | 504 | 121 | 1092 | 893 | 10 |
| C24-LGP3 | 521 | 125 | 1077 | 881 | 10 |
| C24-LGP4 | 536 | 129 | 1064 | 871 | 11 |
| C24-LGP5 | 487 | 117 | 1106 | 905 | 10 |
| C24-LGP6 | 491 | 118 | 1104 | 903 | 10 |
| C24-LGP7 | 497 | 119 | 1098 | 899 | 10 |
| C24-LGP8 | 499 | 120 | 1096 | 897 | 10 |
| C20-BGP1 | 562 | 112 | 1077 | 882 | 17 |
| C20-BGP2 | 577 | 115 | 1065 | 871 | 17 |
| C20-BGP3 | 596 | 119 | 1050 | 859 | 18 |
| C20-BGP4 | 614 | 123 | 1036 | 847 | 18 |
| C20-BGP5 | 554 | 111 | 1084 | 887 | 11 |
| C20-BGP6 | 560 | 112 | 1079 | 883 | 11 |
| C20-BGP7 | 567 | 113 | 1074 | 878 | 14 |
| C20-BGP8 | 569 | 114 | 1071 | 877 | 11 |

*Table 5.16 Mix proportion of concretes with various SBG indices (Cont.)*

| Designation | Cement ($kg/m^3$) | Water ($kg/m^3$) | C. Aggregate ($kg/m^3$) | Sand ($kg/m^3$) | Superplas. ($kg/m^3$) |
|---|---|---|---|---|---|
| C24-BGP1 | 521 | 125 | 1077 | 882 | 10 |
| C24-BGP2 | 536 | 129 | 1065 | 871 | 11 |
| C24-BGP3 | 553 | 133 | 1050 | 859 | 11 |
| C24-BGP4 | 569 | 137 | 1036 | 847 | 14 |
| C24-BGP5 | 514 | 123 | 1084 | 887 | 10 |
| C24-BGP6 | 520 | 125 | 1079 | 883 | 10 |
| C24-BGP7 | 526 | 126 | 1074 | 878 | 11 |
| C24-BGP8 | 528 | 127 | 1071 | 877 | 11 |
| C20-GGP1 | 536 | 107 | 1098 | 898 | 11 |
| C20-GGP2 | 548 | 110 | 1088 | 890 | 11 |
| C20-GGP3 | 565 | 113 | 1074 | 879 | 17 |
| C20-GGP4 | 586 | 117 | 1057 | 865 | 18 |
| C20-GGP5 | 531 | 106 | 1102 | 902 | 11 |
| C20-GGP6 | 534 | 107 | 1100 | 900 | 11 |
| C20-GGP7 | 539 | 108 | 1095 | 896 | 11 |
| C20-GGP8 | 543 | 109 | 1092 | 893 | 14 |
| C24-GGP1 | 498 | 119 | 1098 | 898 | 10 |
| C24-GGP2 | 509 | 122 | 1088 | 890 | 10 |
| C24-GGP3 | 525 | 126 | 1074 | 879 | 10 |
| C24-GGP4 | 544 | 131 | 1057 | 865 | 11 |
| C24-GGP5 | 493 | 118 | 1102 | 902 | 10 |
| C24-GGP6 | 495 | 119 | 1100 | 900 | 10 |
| C24-GGP7 | 501 | 120 | 1095 | 896 | 10 |
| C24-GGP8 | 504 | 121 | 1092 | 893 | 10 |

*Table 5.17 Compressive strength of concrete with various SBG indices*

| Designation | Compressive Strength (MPa) | | | |
|---|---|---|---|---|
| | 7 days | 28 days | 56 days | 91 days |
| C20-LGP1 | 47.65 | 72.52 | 84.11 | 87.37 |
| C20-LGP2 | 48.55 | 75.32 | 86.29 | 90.64 |
| C20-LGP3 | 51.06 | 77.68 | 87.94 | 93.66 |
| C20-LGP4 | 54.11 | 81.57 | 90.42 | 95.06 |
| C20-LGP5 | 46.55 | 72.61 | 80.72 | 87.08 |
| C20-LGP6 | 47.17 | 74.48 | 83.66 | 89.64 |
| C20-LGP7 | 49.11 | 78.93 | 85.19 | 89.13 |
| C20-LGP8 | 48.36 | 81.26 | 86.07 | 91.20 |

*Table 5.17 Compressive strength of concrete with various SBG indices (Cont.)*

| Designation | Compressive Strength (MPa) | | | |
|---|---|---|---|---|
| | 7 days | 28 days | 56 days | 91 days |
| C24-LGP1 | 39.21 | 64.16 | 72.33 | 80.12 |
| C24-LGP2 | 42.55 | 66.23 | 75.39 | 82.63 |
| C24-LGP3 | 40.19 | 69.52 | 77.43 | 84.07 |
| C24-LGP4 | 46.84 | 71.36 | 80.22 | 85.18 |
| C24-LGP5 | 36.72 | 60.19 | 70.62 | 78.11 |
| C24-LGP6 | 38.25 | 63.84 | 71.40 | 77.93 |
| C24-LGP7 | 39.17 | 64.20 | 73.18 | 80.61 |
| C24-LGP8 | 40.29 | 66.11 | 75.95 | 82.44 |
| C20-BGP1 | 57.84 | 90.67 | 98.12 | 104.30 |
| C20-BGP2 | 60.84 | 92.88 | 101.46 | 106.28 |
| C20-BGP3 | 60.03 | 94.00 | 104.80 | 110.75 |
| C20-BGP4 | 62.14 | 94.66 | 107.20 | 113.48 |
| C20-BGP5 | 55.11 | 87.35 | 108.33 | 115.81 |
| C20-BGP6 | 57.47 | 89.62 | 107.54 | 112.03 |
| C20-BGP7 | 58.90 | 91.79 | 110.15 | 114.74 |
| C20-BGP8 | 60.11 | 93.54 | 112.25 | 117.93 |
| C24-BGP1 | 45.12 | 78.03 | 85.43 | 89.64 |
| C24-BGP2 | 47.39 | 77.12 | 88.09 | 92.33 |
| C24-BGP3 | 48.05 | 81.64 | 90.61 | 95.40 |
| C24-BGP4 | 51.63 | 82.49 | 92.27 | 97.12 |
| C24-BGP5 | 44.58 | 74.52 | 82.31 | 85.29 |
| C24-BGP6 | 46.16 | 77.12 | 85.84 | 88.40 |
| C24-BGP7 | 47.94 | 79.63 | 86.15 | 92.13 |
| C24-BGP8 | 45.62 | 80.44 | 88.27 | 93.44 |
| C20-GGP1 | 46.30 | 72.77 | 85.39 | 93.50 |
| C20-GGP2 | 48.52 | 74.13 | 86.11 | 96.27 |
| C20-GGP3 | 48.64 | 75.42 | 90.62 | 98.60 |
| C20-GGP4 | 49.04 | 74.92 | 89.43 | 99.43 |
| C20-GGP5 | 44.82 | 70.98 | 85.18 | 88.73 |
| C20-GGP6 | 46.15 | 73.99 | 88.79 | 94.48 |
| C20-GGP7 | 46.11 | 75.28 | 90.37 | 96.12 |
| C20-GGP8 | 48.84 | 75.97 | 91.16 | 95.48 |
| C24-GGP1 | 38.45 | 60.81 | 69.25 | 77.25 |
| C24-GGP2 | 37.03 | 61.27 | 72.14 | 78.34 |
| C24-GGP3 | 40.15 | 63.94 | 73.61 | 80.05 |
| C24-GGP4 | 42.67 | 65.13 | 74.84 | 81.23 |
| C24-GGP5 | 34.15 | 58.43 | 68.55 | 75.46 |
| C24-GGP6 | 35.22 | 60.13 | 69.72 | 77.82 |
| C24-GGP7 | 37.53 | 61.43 | 71.08 | 79.54 |
| C24-GGP8 | 36.89 | 60.55 | 72.17 | 80.66 |

*Table 5.18 Magnifying coefficients corresponding to strength indices*

| Strength Index | $S_{i,ACV}$ | $S_{i,AIV}$ | $S_{i,MLAA}$ | $S_{i,PLS}$ |
|---|---|---|---|---|
| Magnifying Coefficient (c) | 2.53 | 1.89 | 2.09 | 0.18 |

*Table 5.19 Packing density and SBG indices of various coarse aggregates*

| Rock Type | Gradation Pattern | Packing Density | SBG Index | | | |
|---|---|---|---|---|---|---|
| | | | $S_{i,ACV}$ | $S_{i,AIV}$ | $S_{i,MLAA}$ | $S_{i,PLS}$ |
| Limestone A | No. 1 | 0.6271 | 0.2861 | 0.3561 | 0.2291 | 0.5480 |
| | No. 2 | 0.6115 | 0.2971 | 0.3690 | 0.2375 | 0.5713 |
| | No. 3 | 0.5894 | 0.3085 | 0.3807 | 0.2393 | 0.5882 |
| | No. 4 | 0.5677 | 0.3281 | 0.3854 | 0.2416 | 0.5951 |
| | No. 5 | 0.6338 | 0.2780 | 0.3465 | 0.2227 | 0.5699 |
| | No. 6 | 0.6281 | 0.2808 | 0.3504 | 0.2300 | 0.5714 |
| | No. 7 | 0.6193 | 0.2841 | 0.3573 | 0.2350 | 0.5758 |
| | No. 8 | 0.6195 | 0.2977 | 0.3656 | 0.2365 | 0.5815 |
| Basalt A | No. 1 | 0.5929 | 0.3136 | 0.3972 | 0.2629 | 0.5603 |
| | No. 2 | 0.5766 | 0.3338 | 0.4090 | 0.2683 | 0.5820 |
| | No. 3 | 0.5562 | 0.3457 | 0.4130 | 0.2690 | 0.6034 |
| | No. 4 | 0.5384 | 0.3592 | 0.4058 | 0.2706 | 0.6174 |
| | No. 5 | 0.5973 | 0.2980 | 0.3860 | 0.2570 | 0.5736 |
| | No. 6 | 0.5893 | 0.3075 | 0.3916 | 0.2613 | 0.5720 |
| | No. 7 | 0.5863 | 0.3156 | 0.3999 | 0.2630 | 0.5750 |
| | No. 8 | 0.5900 | 0.3284 | 0.4051 | 0.2664 | 0.5801 |
| Granite A | No. 1 | 0.6174 | 0.2927 | 0.3288 | 0.2409 | 0.5384 |
| | No. 2 | 0.6034 | 0.3025 | 0.3405 | 0.2484 | 0.5562 |
| | No. 3 | 0.5820 | 0.3104 | 0.3452 | 0.2487 | 0.5766 |
| | No. 4 | 0.5603 | 0.3137 | 0.3507 | 0.2489 | 0.5929 |
| | No. 5 | 0.6201 | 0.2838 | 0.3185 | 0.2340 | 0.5500 |
| | No. 6 | 0.6150 | 0.2870 | 0.3286 | 0.2387 | 0.5463 |
| | No. 7 | 0.6120 | 0.2963 | 0.3317 | 0.2415 | 0.5493 |
| | No. 8 | 0.6136 | 0.2992 | 0.3317 | 0.2458 | 0.5573 |

*Table 5.20 Packing density of each size of fine and coarse aggregates*

| Fine Aggregate | | | Coarse Aggregate | | | |
|---|---|---|---|---|---|---|
| Passing Sieve No. | Max. Diam. (mm) | Packing Density | Max. Diam. (mm) | Packing Density | | |
| | | | | Limestone | Basalt | Granite |
| 3/8" | 0.53 | 0.5602 | 25.40 | 0.5904 | 0.5664 | 0.5818 |
| 4 | 4.75 | 0.5652 | 19.05 | 0.5861 | 0.5509 | 0.5806 |
| 8 | 2.36 | 0.5730 | 12.70 | 0.5717 | 0.5416 | 0.5717 |
| 16 | 1.18 | 0.5739 | 9.53 | 0.5477 | 0.5384 | 0.5603 |
| 30 | 0.60 | 0.5776 | | | | |
| 50 | 0.30 | 0.5805 | | | | |
| 100 | 0.15 | 0.5847 | | | | |

*Table 5.21 Optimum S/A ratio and maximum packing density obtained from calculation of various aggregate mixtures*

| Gradation | | Limestone | | Basalt | | Granite | |
|---|---|---|---|---|---|---|---|
| Coarse Aggregate | Fine Aggregate | Optimum S/A Ratio | Maximum Packing | Optimum S/A Ratio | Maximum Packing | Optimum S/A Ratio | Maximum Packing |
| GP01 | FM 2.15 | 0.37 | 0.7406 | 0.41 | 0.7283 | 0.37 | 0.7409 |
| | FM 2.45 | 0.39 | 0.7392 | 0.43 | 0.7273 | 0.39 | 0.7395 |
| | FM 2.74 | 0.41 | 0.7365 | 0.46 | 0.7249 | 0.41 | 0.7368 |
| | FM 3.04 | 0.43 | 0.7318 | 0.48 | 0.7205 | 0.42 | 0.7322 |
| | FM 3.33 | 0.43 | 0.7246 | 0.50 | 0.7131 | 0.43 | 0.7249 |
| GP02 | FM 2.15 | 0.40 | 0.7327 | 0.44 | 0.7211 | 0.40 | 0.7343 |
| | FM 2.45 | 0.42 | 0.7315 | 0.47 | 0.7203 | 0.42 | 0.7331 |
| | FM 2.74 | 0.45 | 0.7290 | 0.50 | 0.7182 | 0.44 | 0.7305 |
| | FM 3.04 | 0.47 | 0.7244 | 0.53 | 0.7139 | 0.46 | 0.7259 |
| | FM 3.33 | 0.48 | 0.7170 | 0.55 | 0.7066 | 0.47 | 0.7185 |
| GP03 | FM 2.15 | 0.45 | 0.7225 | 0.49 | 0.7138 | 0.44 | 0.7256 |
| | FM 2.45 | 0.48 | 0.7216 | 0.52 | 0.7134 | 0.47 | 0.7247 |
| | FM 2.74 | 0.51 | 0.7195 | 0.56 | 0.7117 | 0.49 | 0.7224 |
| | FM 3.04 | 0.54 | 0.7152 | 0.59 | 0.7078 | 0.52 | 0.7180 |
| | FM 3.33 | 0.55 | 0.7078 | 0.61 | 0.7005 | 0.53 | 0.7105 |
| GP04 | FM 2.15 | 0.51 | 0.7120 | 0.53 | 0.7082 | 0.49 | 0.7174 |
| | FM 2.45 | 0.55 | 0.7118 | 0.57 | 0.7082 | 0.52 | 0.7169 |
| | FM 2.74 | 0.58 | 0.7102 | 0.61 | 0.7069 | 0.55 | 0.7150 |
| | FM 3.04 | 0.62 | 0.7064 | 0.65 | 0.7034 | 0.58 | 0.7109 |
| | FM 3.33 | 0.64 | 0.6993 | 0.68 | 0.6964 | 0.60 | 0.7036 |
| GP05 | FM 2.15 | 0.35 | 0.7447 | 0.39 | 0.7322 | 0.35 | 0.7441 |
| | FM 2.45 | 0.37 | 0.7433 | 0.42 | 0.7311 | 0.37 | 0.7427 |
| | FM 2.74 | 0.39 | 0.7406 | 0.44 | 0.7287 | 0.39 | 0.7401 |
| | FM 3.04 | 0.41 | 0.7361 | 0.46 | 0.7243 | 0.41 | 0.7355 |
| | FM 3.33 | 0.41 | 0.7290 | 0.47 | 0.7171 | 0.41 | 0.7284 |
| GP06 | FM 2.15 | 0.36 | 0.7423 | 0.41 | 0.7289 | 0.36 | 0.7420 |
| | FM 2.45 | 0.38 | 0.7411 | 0.43 | 0.7280 | 0.38 | 0.7407 |
| | FM 2.74 | 0.40 | 0.7384 | 0.46 | 0.7258 | 0.40 | 0.7382 |
| | FM 3.04 | 0.42 | 0.7339 | 0.48 | 0.7214 | 0.42 | 0.7336 |
| | FM 3.33 | 0.42 | 0.7268 | 0.49 | 0.7142 | 0.42 | 0.7265 |
| GP07 | FM 2.15 | 0.38 | 0.7386 | 0.42 | 0.7259 | 0.38 | 0.7389 |
| | FM 2.45 | 0.40 | 0.7374 | 0.45 | 0.7251 | 0.40 | 0.7376 |
| | FM 2.74 | 0.42 | 0.7348 | 0.47 | 0.7228 | 0.42 | 0.7350 |
| | FM 3.04 | 0.44 | 0.7302 | 0.50 | 0.7185 | 0.44 | 0.7304 |
| | FM 3.33 | 0.44 | 0.7229 | 0.51 | 0.7112 | 0.44 | 0.7232 |
| GP08 | FM 2.15 | 0.39 | 0.7351 | 0.42 | 0.7248 | 0.38 | 0.7369 |
| | FM 2.45 | 0.41 | 0.7337 | 0.45 | 0.7238 | 0.40 | 0.7354 |
| | FM 2.74 | 0.43 | 0.7310 | 0.48 | 0.7214 | 0.43 | 0.7327 |
| | FM 3.04 | 0.45 | 0.7263 | 0.51 | 0.7170 | 0.45 | 0.7280 |
| | FM 3.33 | 0.46 | 0.7188 | 0.52 | 0.7095 | 0.45 | 0.7205 |

*Table 5.22 Optimum S/A ratio and maximum packing density obtained from experiment of various aggregate mixtures*

| Gradation | | Limestone | | Basalt | | Granite | |
|---|---|---|---|---|---|---|---|
| Coarse Aggregate | Fine Aggregate | Optimum S/A Ratio | Maximum Packing | Optimum S/A Ratio | Maximum Packing | Optimum S/A Ratio | Maximum Packing |
| GP01 | FM 2.15 | 0.40 | 0.7592 | 0.42 | 0.7305 | 0.40 | 0.7548 |
| | FM 2.45 | 0.41 | 0.7418 | 0.44 | 0.7464 | 0.40 | 0.7466 |
| | FM 2.74 | 0.42 | 0.7394 | 0.45 | 0.7428 | 0.42 | 0.7654 |
| | FM 3.04 | 0.44 | 0.7386 | 0.47 | 0.7511 | 0.45 | 0.7512 |
| | FM 3.33 | 0.45 | 0.7511 | 0.49 | 0.7392 | 0.45 | 0.7584 |
| GP02 | FM 2.15 | 0.42 | 0.7504 | 0.45 | 0.7416 | 0.40 | 0.7419 |
| | FM 2.45 | 0.44 | 0.7525 | 0.45 | 0.7502 | 0.43 | 0.7604 |
| | FM 2.74 | 0.45 | 0.7426 | 0.48 | 0.7469 | 0.45 | 0.7493 |
| | FM 3.04 | 0.44 | 0.7382 | 0.51 | 0.7383 | 0.45 | 0.7326 |
| | FM 3.33 | 0.47 | 0.7167 | 0.53 | 0.7304 | 0.44 | 0.7255 |
| GP03 | FM 2.15 | 0.45 | 0.7448 | 0.47 | 0.7256 | 0.42 | 0.7568 |
| | FM 2.45 | 0.48 | 0.7566 | 0.48 | 0.7288 | 0.46 | 0.7352 |
| | FM 2.74 | 0.46 | 0.7402 | 0.52 | 0.7315 | 0.47 | 0.7393 |
| | FM 3.04 | 0.50 | 0.7316 | 0.55 | 0.7312 | 0.50 | 0.7446 |
| | FM 3.33 | 0.50 | 0.7148 | 0.57 | 0.7258 | 0.48 | 0.7293 |
| GP04 | FM 2.15 | 0.50 | 0.7390 | 0.54 | 0.7225 | 0.45 | 0.7255 |
| | FM 2.45 | 0.55 | 0.7414 | 0.55 | 0.7244 | 0.47 | 0.7212 |
| | FM 2.74 | 0.53 | 0.7308 | 0.57 | 0.7318 | 0.49 | 0.7345 |
| | FM 3.04 | 0.55 | 0.7343 | 0.58 | 0.7265 | 0.50 | 0.7334 |
| | FM 3.33 | 0.58 | 0.7166 | 0.55 | 0.7202 | 0.54 | 0.7204 |
| GP05 | FM 2.15 | 0.37 | 0.7512 | 0.41 | 0.7376 | 0.38 | 0.7512 |
| | FM 2.45 | 0.40 | 0.7632 | 0.43 | 0.7245 | 0.40 | 0.7555 |
| | FM 2.74 | 0.42 | 0.7518 | 0.42 | 0.7308 | 0.42 | 0.7612 |
| | FM 3.04 | 0.43 | 0.7620 | 0.45 | 0.7461 | 0.41 | 0.7629 |
| | FM 3.33 | 0.44 | 0.7448 | 0.45 | 0.7354 | 0.44 | 0.7564 |
| GP06 | FM 2.15 | 0.40 | 0.7669 | 0.42 | 0.7243 | 0.39 | 0.7493 |
| | FM 2.45 | 0.40 | 0.7518 | 0.44 | 0.7305 | 0.40 | 0.7558 |
| | FM 2.74 | 0.42 | 0.7561 | 0.45 | 0.7344 | 0.42 | 0.7620 |
| | FM 3.04 | 0.43 | 0.7315 | 0.47 | 0.7410 | 0.44 | 0.7411 |
| | FM 3.33 | 0.45 | 0.7454 | 0.48 | 0.7298 | 0.43 | 0.7413 |
| GP07 | FM 2.15 | 0.40 | 0.7616 | 0.42 | 0.7388 | 0.40 | 0.7512 |
| | FM 2.45 | 0.43 | 0.7593 | 0.43 | 0.7404 | 0.41 | 0.7664 |
| | FM 2.74 | 0.41 | 0.7521 | 0.45 | 0.7325 | 0.42 | 0.7612 |
| | FM 3.04 | 0.45 | 0.7635 | 0.48 | 0.7448 | 0.45 | 0.7455 |
| | FM 3.33 | 0.47 | 0.7469 | 0.50 | 0.7366 | 0.45 | 0.7394 |
| GP08 | FM 2.15 | 0.42 | 0.7481 | 0.43 | 0.7306 | 0.41 | 0.7515 |
| | FM 2.45 | 0.41 | 0.7502 | 0.45 | 0.7225 | 0.42 | 0.7484 |
| | FM 2.74 | 0.45 | 0.7336 | 0.47 | 0.7308 | 0.45 | 0.7606 |
| | FM 3.04 | 0.45 | 0.7550 | 0.50 | 0.7440 | 0.46 | 0.7515 |
| | FM 3.33 | 0.48 | 0.7426 | 0.50 | 0.7312 | 0.47 | 0.7304 |

*Table 5.23 Mix proportion of concrete with various ratio of paste volume to void content of dry and compacted aggregate*

| Designation | Cement ($kg/m^3$) | Water ($kg/m^3$) | C. Aggregate ($kg/m^3$) | Sand ($kg/m^3$) | Superplas. ($kg/m^3$) |
|---|---|---|---|---|---|
| C20-L10-SC10 | 705 | 141 | 862 | 705 | 7 |
| C20-L10-SC12 | 608 | 122 | 930 | 761 | 12 |
| C20-L10-SC15 | 535 | 107 | 981 | 803 | 11 |
| C20-L10-SC17 | 478 | 96 | 1022 | 836 | 14 |
| C20-L10-SC20 | 431 | 86 | 1054 | 862 | 26 |
| C20-L34-SC10 | 705 | 141 | 862 | 705 | 7 |
| C20-L34-SC12 | 608 | 122 | 930 | 761 | 12 |
| C20-L34-SC15 | 535 | 107 | 981 | 803 | 13 |
| C20-L34-SC17 | 478 | 96 | 1022 | 836 | 19 |
| C20-L34-SC20 | 431 | 86 | 1054 | 862 | 22 |
| C20-L12-SC10 | 705 | 141 | 862 | 705 | 7 |
| C20-L12-SC12 | 608 | 122 | 930 | 761 | 15 |
| C20-L12-SC15 | 535 | 107 | 981 | 803 | 16 |
| C20-L12-SC17 | 478 | 96 | 1022 | 836 | 24 |
| C20-L12-SC20 | 431 | 86 | 1054 | 862 | 30 |
| C20-L38-SC10 | 705 | 141 | 862 | 705 | 11 |
| C20-L38-SC12 | 608 | 122 | 930 | 761 | 18 |
| C20-L38-SC15 | 535 | 107 | 981 | 803 | 16 |
| C20-L38-SC17 | 478 | 96 | 1022 | 836 | 24 |
| C20-L38-SC20 | 431 | 86 | 1054 | 862 | 30 |
| C20-B10-SC10 | 775 | 155 | 947 | 775 | 8 |
| C20-B10-SC12 | 674 | 135 | 1030 | 843 | 13 |
| C20-B10-SC15 | 596 | 119 | 1093 | 895 | 12 |
| C20-B10-SC17 | 535 | 107 | 1144 | 936 | 16 |
| C20-B10-SC20 | 485 | 97 | 1185 | 969 | 29 |
| C20-B34-SC10 | 775 | 155 | 947 | 775 | 8 |
| C20-B34-SC12 | 674 | 135 | 1030 | 843 | 13 |
| C20-B34-SC15 | 596 | 119 | 1093 | 895 | 15 |
| C20-B34-SC17 | 535 | 107 | 1144 | 936 | 21 |
| C20-B34-SC20 | 485 | 97 | 1185 | 969 | 24 |

*Table 5.23 Mix proportion of concrete with various ratio of paste volume to void content of dry and compacted aggregate (Cont.)*

| Designation | Cement ($kg/m^3$) | Water ($kg/m^3$) | C. Aggregate ($kg/m^3$) | Sand ($kg/m^3$) | Superplas. ($kg/m^3$) |
|---|---|---|---|---|---|
| C20-B12-SC10 | 775 | 155 | 947 | 775 | 8 |
| C20-B12-SC12 | 674 | 135 | 1030 | 843 | 17 |
| C20-B12-SC15 | 596 | 119 | 1093 | 895 | 18 |
| C20-B12-SC17 | 535 | 107 | 1144 | 936 | 27 |
| C20-B12-SC20 | 485 | 97 | 1185 | 969 | 34 |
| C20-B38-SC10 | 775 | 155 | 947 | 775 | 12 |
| C20-B38-SC12 | 674 | 135 | 1030 | 843 | 20 |
| C20-B38-SC15 | 596 | 119 | 1093 | 895 | 18 |
| C20-B38-SC17 | 535 | 107 | 1144 | 936 | 27 |
| C20-B38-SC20 | 485 | 97 | 1185 | 969 | 34 |
| C20-G10-SC10 | 754 | 151 | 922 | 754 | 8 |
| C20-G10-SC12 | 654 | 131 | 1000 | 818 | 7 |
| C20-G10-SC15 | 578 | 116 | 1059 | 867 | 17 |
| C20-G10-SC17 | 517 | 103 | 1107 | 905 | 16 |
| C20-G10-SC20 | 468 | 94 | 1145 | 937 | 28 |
| C20-G34-SC10 | 754 | 151 | 922 | 754 | 8 |
| C20-G34-SC12 | 654 | 131 | 1000 | 818 | 13 |
| C20-G34-SC15 | 578 | 116 | 1059 | 867 | 12 |
| C20-G34-SC17 | 517 | 103 | 1107 | 905 | 16 |
| C20-G34-SC20 | 468 | 94 | 1145 | 937 | 23 |
| C20-G12-SC10 | 754 | 151 | 922 | 754 | 8 |
| C20-G12-SC12 | 654 | 131 | 1000 | 818 | 16 |
| C20-G12-SC15 | 578 | 116 | 1059 | 867 | 17 |
| C20-G12-SC17 | 517 | 103 | 1107 | 905 | 26 |
| C20-G12-SC20 | 468 | 94 | 1145 | 937 | 33 |
| C20-G38-SC10 | 754 | 151 | 922 | 754 | 11 |
| C20-G38-SC12 | 654 | 131 | 1000 | 818 | 20 |
| C20-G38-SC15 | 578 | 116 | 1059 | 867 | 17 |
| C20-G38-SC17 | 517 | 103 | 1107 | 905 | 26 |
| C20-G38-SC20 | 468 | 94 | 1145 | 937 | 33 |

***Table 5.24*** *Ratio of paste volume to void content of dry and compacted aggregate of concretes*

| Designation | $\gamma$ | Designation | $\gamma$ | Designation | $\gamma$ |
|---|---|---|---|---|---|
| C20-L10-SC10 | 1.56 | C20-B10-SC10 | 1.51 | C20-G10-SC10 | 1.53 |
| C20-L10-SC12 | 1.36 | C20-B10-SC12 | 1.31 | C20-G10-SC12 | 1.33 |
| C20-L10-SC15 | 1.20 | C20-B10-SC15 | 1.16 | C20-G10-SC15 | 1.17 |
| C20-L10-SC17 | 1.07 | C20-B10-SC17 | 1.04 | C20-G10-SC17 | 1.05 |
| C20-L10-SC20 | 0.97 | C20-B10-SC20 | 0.94 | C20-G10-SC20 | 0.95 |
| C20-L34-SC10 | 1.53 | C20-B34-SC10 | 1.47 | C20-G34-SC10 | 1.50 |
| C20-L34-SC12 | 1.33 | C20-B34-SC12 | 1.27 | C20-G34-SC12 | 1.30 |
| C20-L34-SC15 | 1.17 | C20-B34-SC15 | 1.13 | C20-G34-SC15 | 1.15 |
| C20-L34-SC17 | 1.05 | C20-B34-SC17 | 1.01 | C20-G34-SC17 | 1.03 |
| C20-L34-SC20 | 0.95 | C20-B34-SC20 | 0.91 | C20-G34-SC20 | 0.93 |
| C20-L12-SC10 | 1.49 | C20-B12-SC10 | 1.42 | C20-G12-SC10 | 1.46 |
| C20-L12-SC12 | 1.29 | C20-B12-SC12 | 1.24 | C20-G12-SC12 | 1.26 |
| C20-L12-SC15 | 1.14 | C20-B12-SC15 | 1.09 | C20-G12-SC15 | 1.11 |
| C20-L12-SC17 | 1.02 | C20-B12-SC17 | 0.98 | C20-G12-SC17 | 1.00 |
| C20-L12-SC20 | 0.92 | C20-B12-SC20 | 0.89 | C20-G12-SC20 | 0.90 |
| C20-L38-SC10 | 1.45 | C20-B38-SC10 | 1.38 | C20-G38-SC10 | 1.41 |
| C20-L38-SC12 | 1.26 | C20-B38-SC12 | 1.20 | C20-G38-SC12 | 1.22 |
| C20-L38-SC15 | 1.11 | C20-B38-SC15 | 1.06 | C20-G38-SC15 | 1.07 |
| C20-L38-SC17 | 0.99 | C20-B38-SC17 | 0.95 | C20-G38-SC17 | 0.96 |
| C20-L38-SC20 | 0.90 | C20-B38-SC20 | 0.86 | C20-G38-SC20 | 0.87 |

***Table 5.25*** *Total porosity of concrete with various ratio of paste volume to void content of dry and compacted aggregate*

| Designation | Total Porosity (%) | | | |
|---|---|---|---|---|
| | 7 days | 28 days | 56 days | 91 days |
| C20-L10-SC10 | 10.20 | 9.27 | 8.73 | 8.46 |
| C20-L10-SC12 | 9.23 | 8.64 | 8.11 | 7.93 |
| C20-L10-SC15 | 8.89 | 8.33 | 7.75 | 7.43 |
| C20-L10-SC17 | 8.53 | 7.86 | 7.37 | 7.12 |
| C20-L10-SC20 | 9.83 | 8.95 | 8.48 | 8.15 |
| C20-L34-SC10 | 10.03 | 9.32 | 8.64 | 8.32 |
| C20-L34-SC12 | 9.06 | 8.52 | 8.03 | 7.76 |
| C20-L34-SC15 | 8.47 | 8.06 | 7.59 | 7.32 |
| C20-L34-SC17 | 8.12 | 7.73 | 7.42 | 7.16 |
| C20-L34-SC20 | 10.73 | 9.60 | 9.15 | 8.84 |
| C20-L12-SC10 | 9.65 | 8.94 | 8.56 | 8.31 |
| C20-L12-SC12 | 8.90 | 8.45 | 8.02 | 7.74 |
| C20-L12-SC15 | 8.41 | 7.89 | 7.52 | 7.29 |
| C20-L12-SC17 | 9.02 | 8.17 | 7.70 | 7.48 |
| C20-L12-SC20 | 11.04 | 10.36 | 9.80 | 9.51 |
| C20-L38-SC10 | 9.40 | 9.09 | 8.65 | 8.27 |
| C20-L38-SC12 | 8.93 | 8.32 | 7.88 | 7.62 |
| C20-L38-SC15 | 8.53 | 8.04 | 7.57 | 7.24 |
| C20-L38-SC17 | 9.25 | 8.56 | 8.02 | 7.88 |
| C20-L38-SC20 | 11.21 | 10.65 | 10.14 | 9.86 |
| C20-B10-SC10 | 9.85 | 9.13 | 8.74 | 8.45 |
| C20-B10-SC12 | 9.17 | 8.29 | 7.90 | 7.63 |
| C20-B10-SC15 | 8.61 | 7.86 | 7.45 | 7.19 |
| C20-B10-SC17 | 8.42 | 7.92 | 7.44 | 7.12 |
| C20-B10-SC20 | 10.72 | 9.68 | 9.05 | 8.47 |
| C20-B34-SC10 | 9.79 | 8.89 | 8.26 | 8.31 |
| C20-B34-SC12 | 9.09 | 8.32 | 7.94 | 7.69 |
| C20-B34-SC15 | 8.47 | 7.76 | 7.25 | 7.22 |
| C20-B34-SC17 | 8.82 | 8.13 | 7.48 | 7.33 |
| C20-B34-SC20 | 11.39 | 10.32 | 9.50 | 9.32 |

*Table 5.25 Total porosity of concrete with various ratio of paste volume to void content of dry and compacted aggregate (Cont.)*

| Designation | Total Porosity (%) | | | |
|---|---|---|---|---|
| | 7 days | 28 days | 56 days | 91 days |
| C20-B12-SC10 | 9.58 | 8.97 | 8.33 | 8.12 |
| C20-B12-SC12 | 8.96 | 8.24 | 7.80 | 7.69 |
| C20-B12-SC15 | 8.38 | 7.74 | 7.43 | 7.20 |
| C20-B12-SC17 | 9.06 | 8.33 | 7.99 | 7.64 |
| C20-B12-SC20 | 11.73 | 10.46 | 10.27 | 9.94 |
| C20-B38-SC10 | 9.22 | 8.59 | 8.06 | 7.82 |
| C20-B38-SC12 | 8.62 | 8.10 | 7.54 | 7.33 |
| C20-B38-SC15 | 8.26 | 7.85 | 7.39 | 7.21 |
| C20-B38-SC17 | 9.84 | 9.34 | 8.87 | 8.52 |
| C20-B38-SC20 | 12.47 | 11.77 | 11.24 | 10.88 |
| C20-G10-SC10 | 9.79 | 9.06 | 8.59 | 8.31 |
| C20-G10-SC12 | 9.42 | 8.73 | 8.16 | 7.96 |
| C20-G10-SC15 | 8.70 | 8.05 | 7.47 | 7.16 |
| C20-G10-SC17 | 8.52 | 7.93 | 7.22 | 7.03 |
| C20-G10-SC20 | 10.45 | 9.71 | 9.35 | 9.04 |
| C20-G34-SC10 | 9.62 | 8.93 | 8.42 | 8.27 |
| C20-G34-SC12 | 9.21 | 8.64 | 8.36 | 8.01 |
| C20-G34-SC15 | 8.66 | 8.05 | 7.69 | 7.54 |
| C20-G34-SC17 | 8.42 | 7.76 | 7.35 | 7.29 |
| C20-G34-SC20 | 10.34 | 9.86 | 9.14 | 8.83 |
| C20-G12-SC10 | 9.69 | 8.92 | 8.26 | 7.95 |
| C20-G12-SC12 | 8.95 | 8.31 | 7.94 | 7.72 |
| C20-G12-SC15 | 8.28 | 7.83 | 7.50 | 7.38 |
| C20-G12-SC17 | 8.84 | 8.04 | 7.82 | 7.41 |
| C20-G12-SC20 | 11.24 | 10.35 | 9.88 | 9.65 |
| C20-G38-SC10 | 9.51 | 8.83 | 8.26 | 8.02 |
| C20-G38-SC12 | 8.78 | 8.15 | 7.54 | 7.30 |
| C20-G38-SC15 | 8.15 | 7.93 | 7.32 | 7.24 |
| C20-G38-SC17 | 10.43 | 9.36 | 8.95 | 8.51 |
| C20-G38-SC20 | 12.61 | 11.13 | 10.62 | 10.28 |

*Table 5.26 Compressive strength of concrete with various ratio of paste volume to void content of dry and compacted aggregate*

| Designation | Compressive Strength (MPa) | | | |
|---|---|---|---|---|
| | 7 days | 28 days | 56 days | 91 days |
| C20-L10-SC10 | 98.14 | 119.82 | 125.23 | 128.95 |
| C20-L10-SC12 | 112.45 | 135.18 | 141.66 | 143.72 |
| C20-L10-SC15 | 123.59 | 144.11 | 152.93 | 155.62 |
| C20-L10-SC17 | 125.72 | 149.37 | 160.54 | 163.42 |
| C20-L10-SC20 | 120.60 | 137.88 | 147.11 | 149.63 |
| C20-L34-SC10 | 102.11 | 124.06 | 131.45 | 137.23 |
| C20-L34-SC12 | 115.62 | 138.91 | 143.66 | 146.95 |
| C20-L34-SC15 | 120.71 | 149.07 | 156.12 | 162.90 |
| C20-L34-SC17 | 121.64 | 153.78 | 159.43 | 164.26 |
| C20-L34-SC20 | 113.48 | 133.45 | 142.68 | 145.41 |
| C20-L12-SC10 | 107.61 | 128.06 | 134.62 | 138.11 |
| C20-L12-SC12 | 112.43 | 143.61 | 148.69 | 152.63 |
| C20-L12-SC15 | 123.50 | 153.16 | 157.13 | 162.86 |
| C20-L12-SC17 | 124.79 | 155.04 | 159.52 | 165.36 |
| C20-L12-SC20 | 110.35 | 126.49 | 132.11 | 137.30 |
| C20-L38-SC10 | 108.64 | 134.18 | 139.31 | 145.23 |
| C20-L38-SC12 | 113.25 | 148.55 | 147.52 | 151.46 |
| C20-L38-SC15 | 122.68 | 157.74 | 161.38 | 164.73 |
| C20-L38-SC17 | 125.19 | 155.55 | 158.15 | 161.28 |
| C20-L38-SC20 | 103.50 | 119.52 | 127.24 | 134.17 |
| C20-B10-SC10 | 105.38 | 129.71 | 132.52 | 135.63 |
| C20-B10-SC12 | 111.47 | 144.94 | 150.17 | 153.18 |
| C20-B10-SC15 | 118.93 | 155.76 | 161.43 | 165.14 |
| C20-B10-SC17 | 120.57 | 156.71 | 163.29 | 166.72 |
| C20-B10-SC20 | 105.76 | 125.98 | 134.56 | 141.45 |
| C20-B34-SC10 | 112.56 | 136.77 | 142.50 | 145.14 |
| C20-B34-SC12 | 120.28 | 146.43 | 151.73 | 156.28 |
| C20-B34-SC15 | 124.37 | 151.22 | 156.84 | 159.35 |
| C20-B34-SC17 | 125.66 | 153.50 | 161.46 | 166.13 |
| C20-B34-SC20 | 110.48 | 129.65 | 138.32 | 145.24 |

***Table 5.26*** *Compressive strength of concrete with various ratio of paste volume to void content of dry and compacted aggregate (Cont.)*

| Designation | Compressive Strength (MPa) | | | |
|---|---|---|---|---|
| | 7 days | 28 days | 56 days | 91 days |
| C20-B12-SC10 | 115.56 | 145.13 | 142.36 | 146.53 |
| C20-B12-SC12 | 122.18 | 154.76 | 159.14 | 158.61 |
| C20-B12-SC15 | 125.74 | 161.80 | 163.24 | 164.80 |
| C20-B12-SC17 | 121.69 | 154.66 | 158.13 | 160.12 |
| C20-B12-SC20 | 108.95 | 121.17 | 130.44 | 138.50 |
| C20-B38-SC10 | 112.46 | 143.57 | 146.27 | 148.32 |
| C20-B38-SC12 | 117.20 | 153.25 | 159.83 | 160.24 |
| C20-B38-SC15 | 128.34 | 161.88 | 165.14 | 168.45 |
| C20-B38-SC17 | 121.07 | 150.85 | 148.35 | 152.58 |
| C20-B38-SC20 | 102.93 | 122.69 | 128.35 | 133.63 |
| C20-G10-SC10 | 103.92 | 124.88 | 131.56 | 135.72 |
| C20-G10-SC12 | 112.88 | 140.60 | 146.39 | 150.93 |
| C20-G10-SC15 | 124.63 | 151.30 | 157.62 | 158.21 |
| C20-G10-SC17 | 126.12 | 156.18 | 160.24 | 164.13 |
| C20-G10-SC20 | 106.47 | 135.22 | 141.88 | 143.32 |
| C20-G34-SC10 | 104.75 | 129.24 | 134.61 | 137.32 |
| C20-G34-SC12 | 115.80 | 145.18 | 151.32 | 155.24 |
| C20-G34-SC15 | 117.42 | 155.02 | 158.25 | 160.35 |
| C20-G34-SC17 | 120.52 | 157.57 | 161.63 | 163.45 |
| C20-G34-SC20 | 106.50 | 131.30 | 137.82 | 141.93 |
| C20-G12-SC10 | 108.13 | 134.42 | 140.43 | 145.21 |
| C20-G12-SC12 | 124.61 | 148.55 | 156.25 | 157.67 |
| C20-G12-SC15 | 127.23 | 155.76 | 160.25 | 163.52 |
| C20-G12-SC17 | 123.25 | 147.09 | 153.73 | 157.12 |
| C20-G12-SC20 | 104.62 | 123.07 | 131.64 | 136.42 |
| C20-G38-SC10 | 108.73 | 134.54 | 140.66 | 145.73 |
| C20-G38-SC12 | 118.31 | 147.71 | 153.73 | 158.66 |
| C20-G38-SC15 | 123.63 | 155.02 | 162.15 | 165.32 |
| C20-G38-SC17 | 115.82 | 140.41 | 147.20 | 148.40 |
| C20-G38-SC20 | 106.23 | 128.64 | 127.31 | 134.29 |

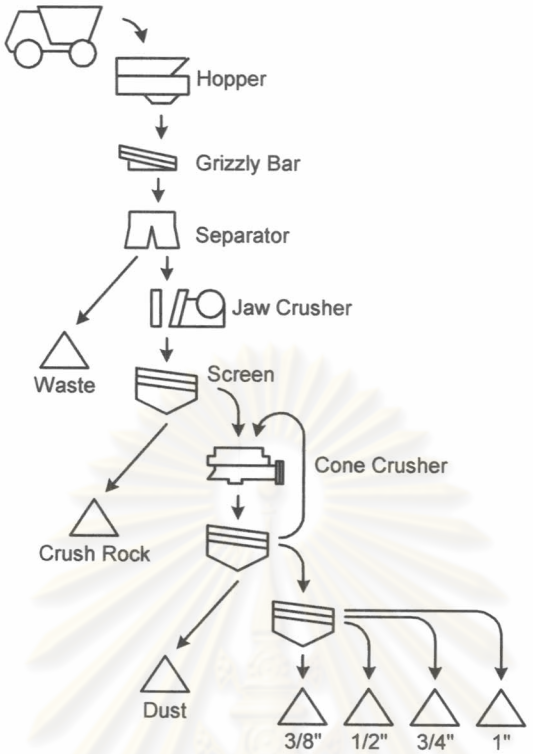


*Fig. 5.1 Schematic diagram for comminution process of rock*

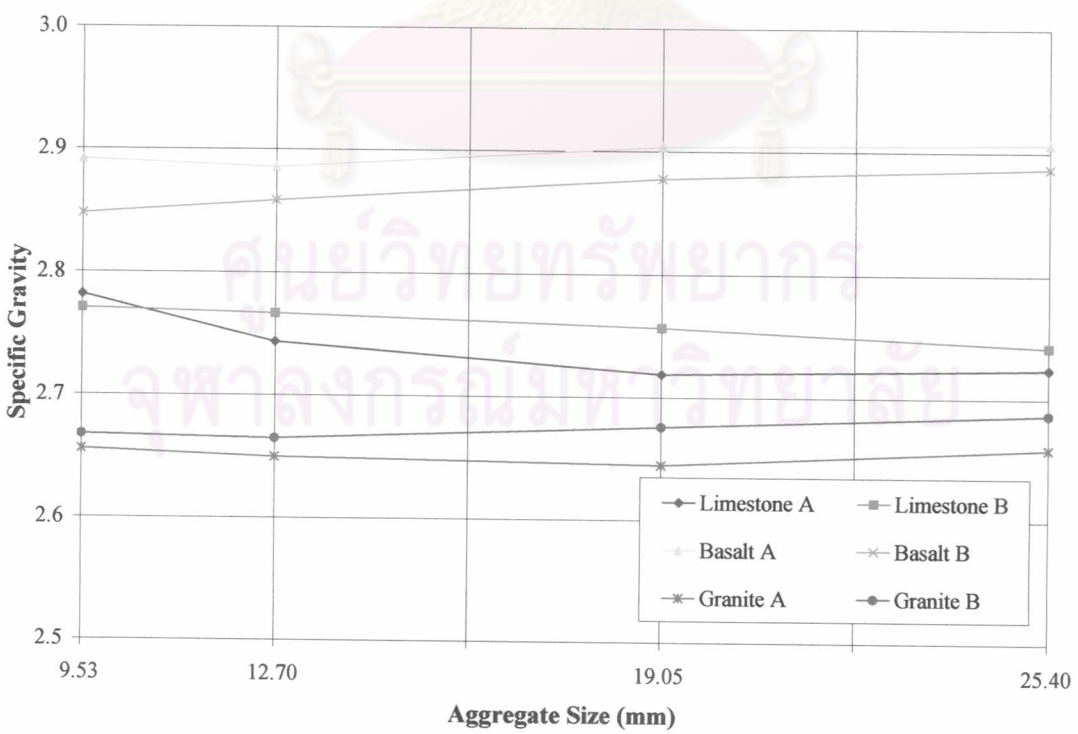


*Fig. 5.2 Specific gravity of coarse aggregates with various sizes*

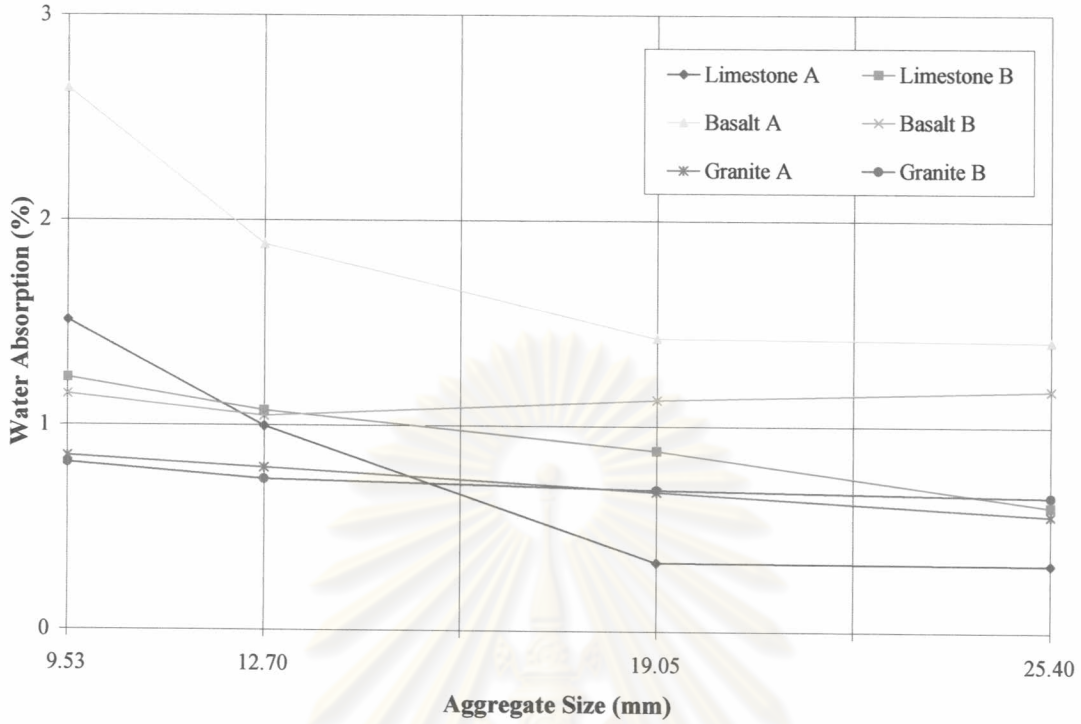


*Fig. 5.3 Water absorption of coarse aggregates with various sizes*

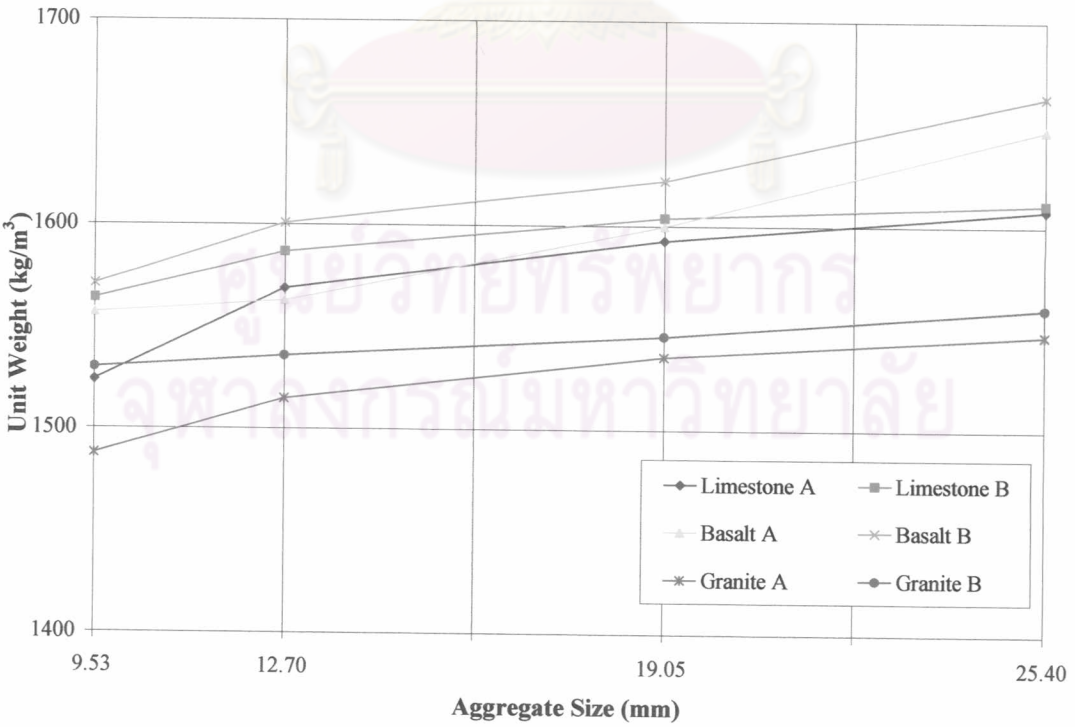


*Fig. 5.4 Unit weight of coarse aggregates with various sizes*

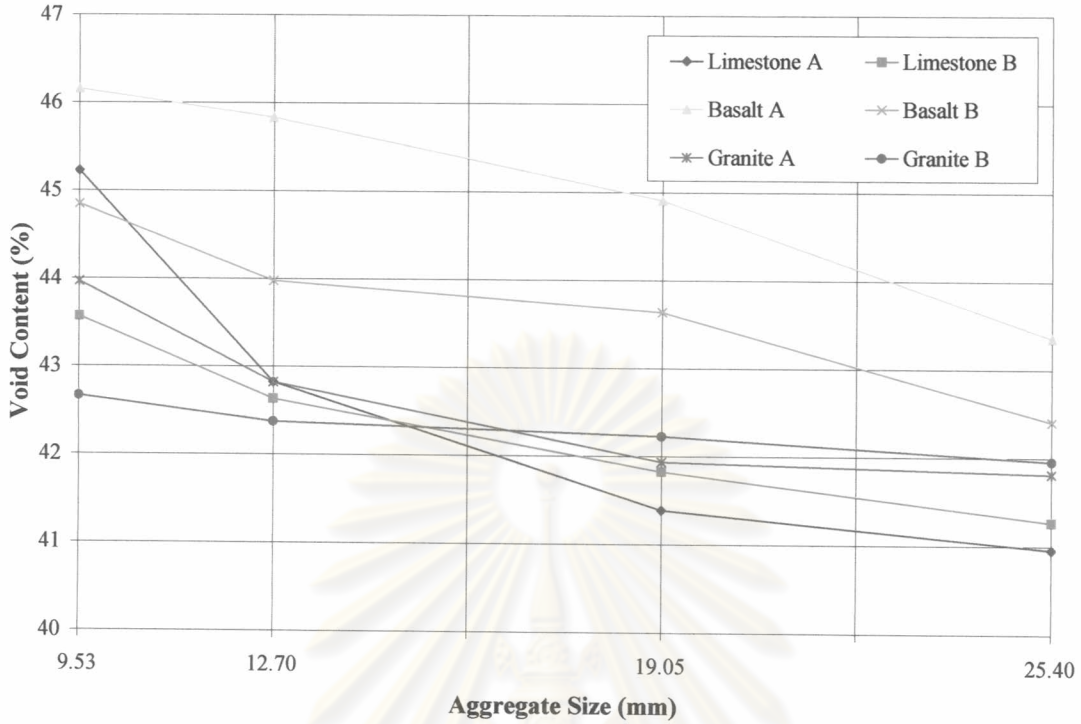


***Fig. 5.5*** *Void content of coarse aggregates with various sizes*

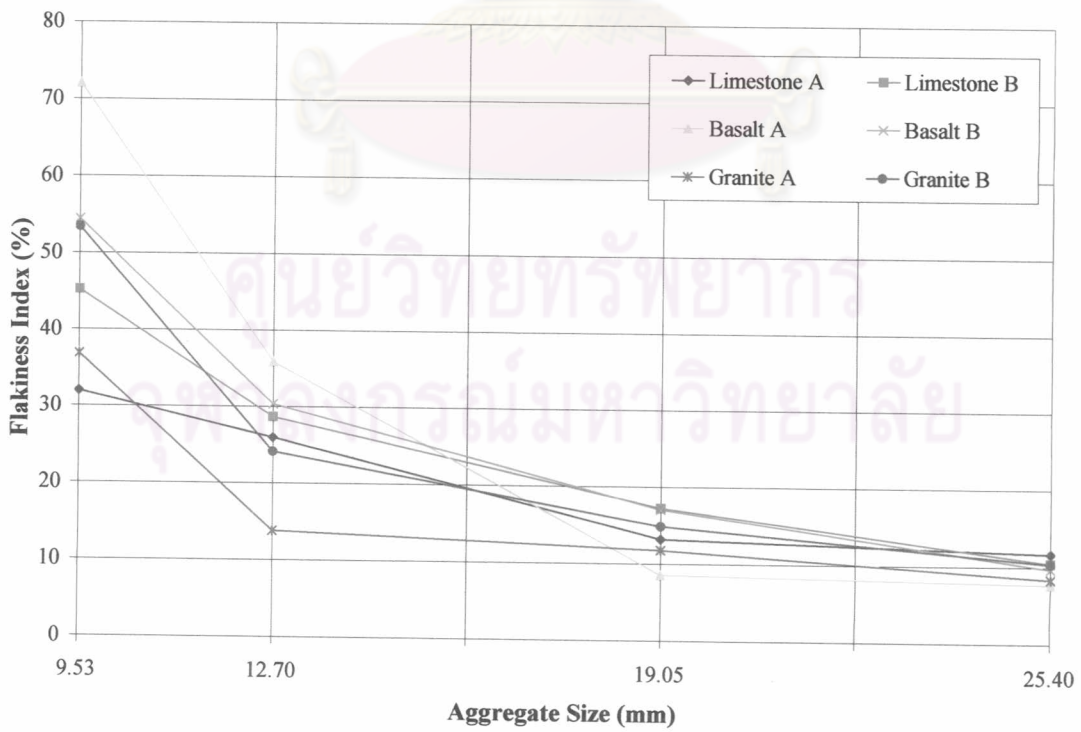


***Fig. 5.6*** *Flakiness index of coarse aggregates with various sizes*

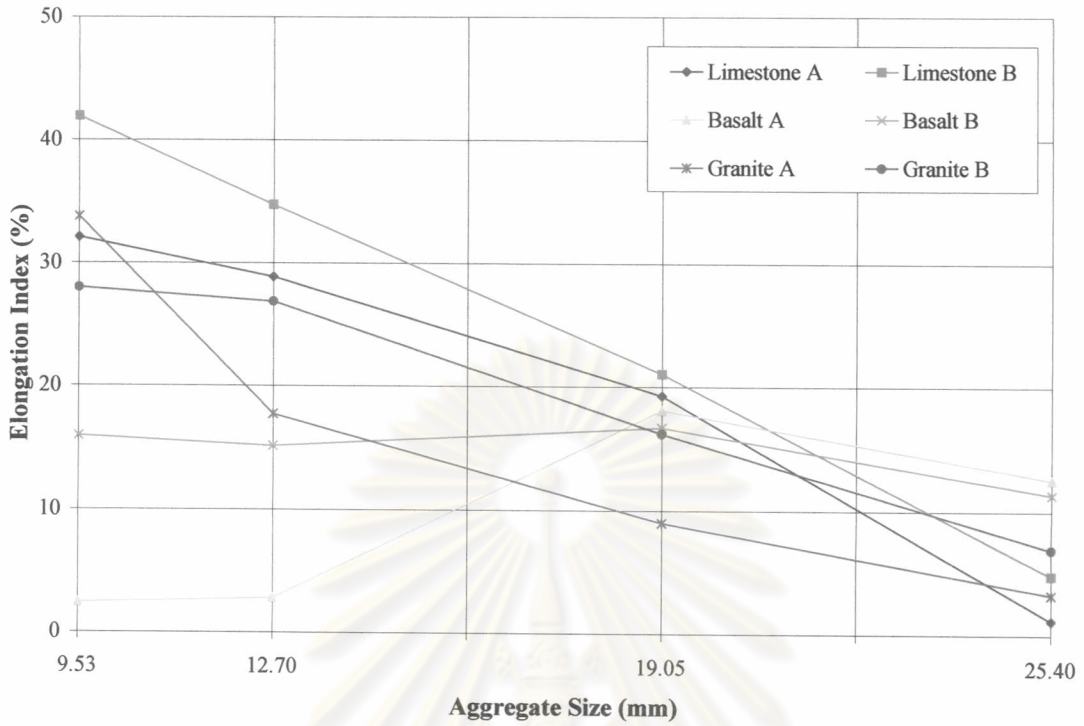


*Fig. 5.7 Elongation index of coarse aggregates with various sizes*

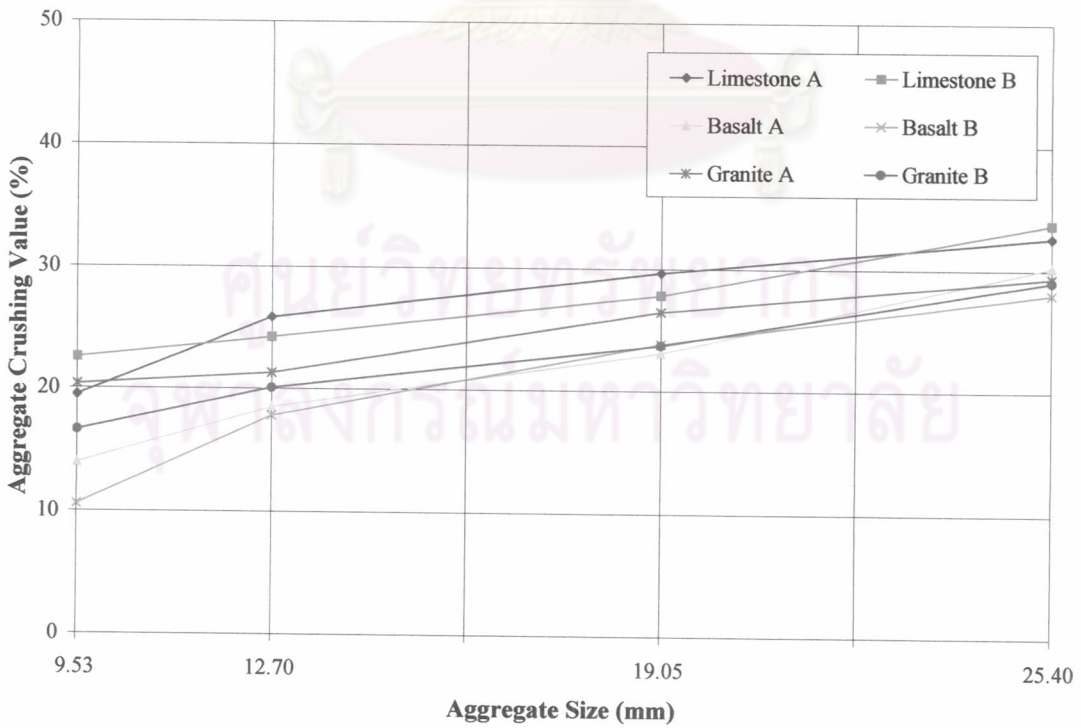


*Fig. 5.8 Aggregate crushing value of coarse aggregates with various sizes*

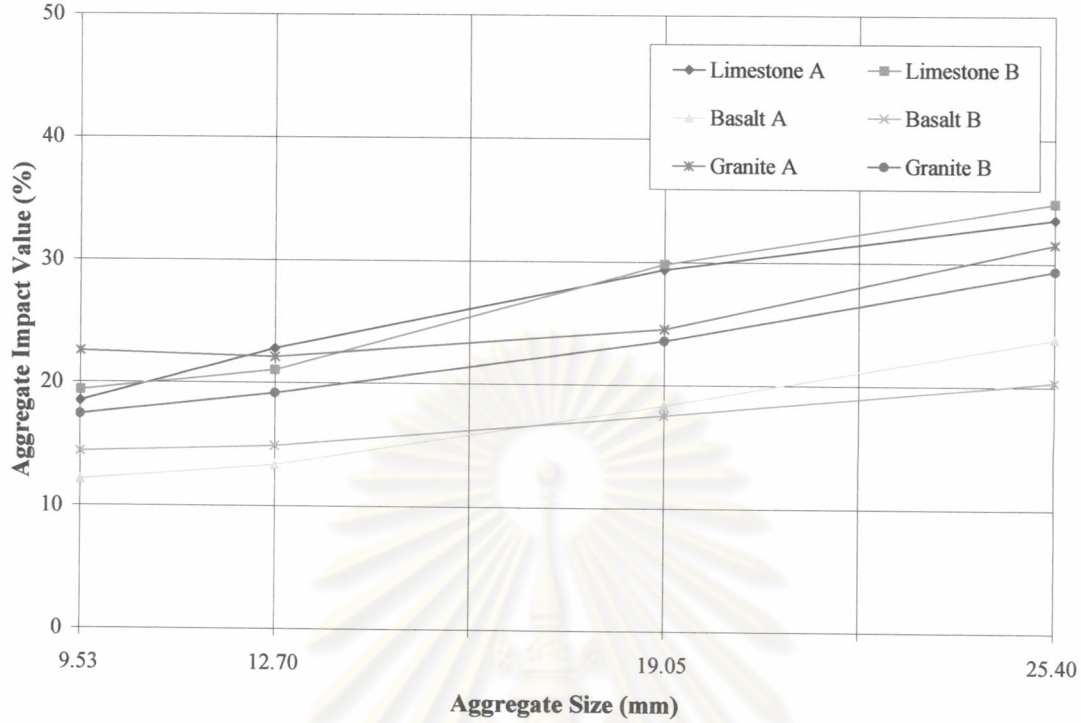


***Fig. 5.9*** *Aggregate impact value of coarse aggregates with various sizes*

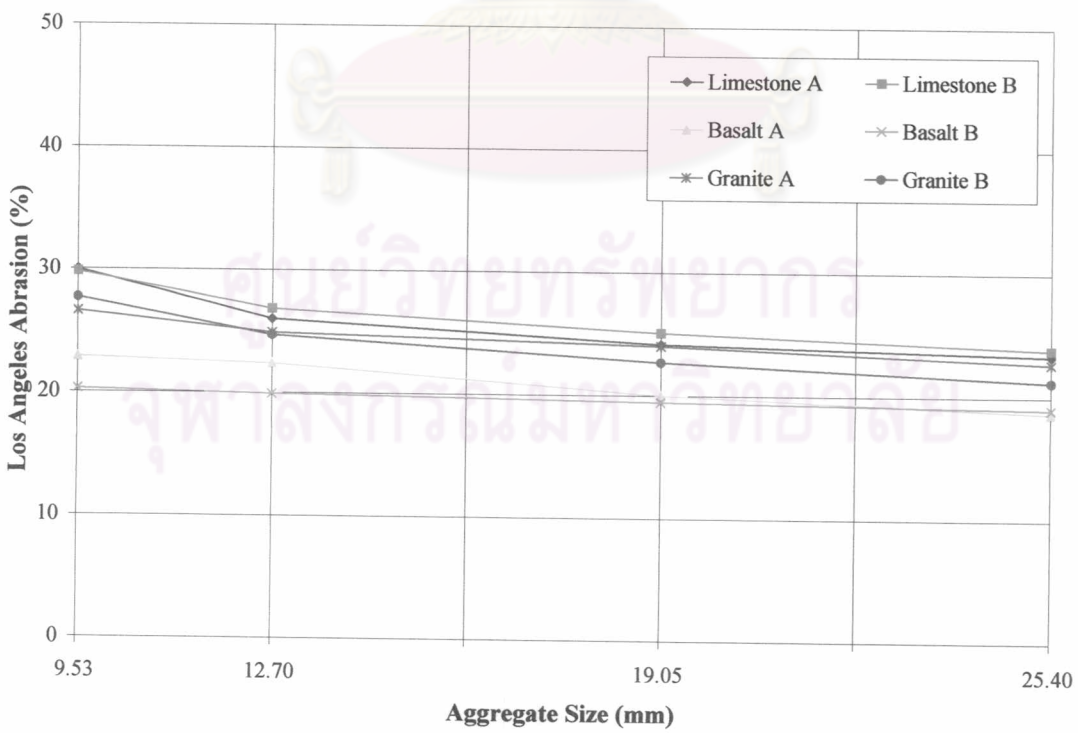


***Fig. 5.10*** *Los Angeles abrasion of coarse aggregates with various sizes*

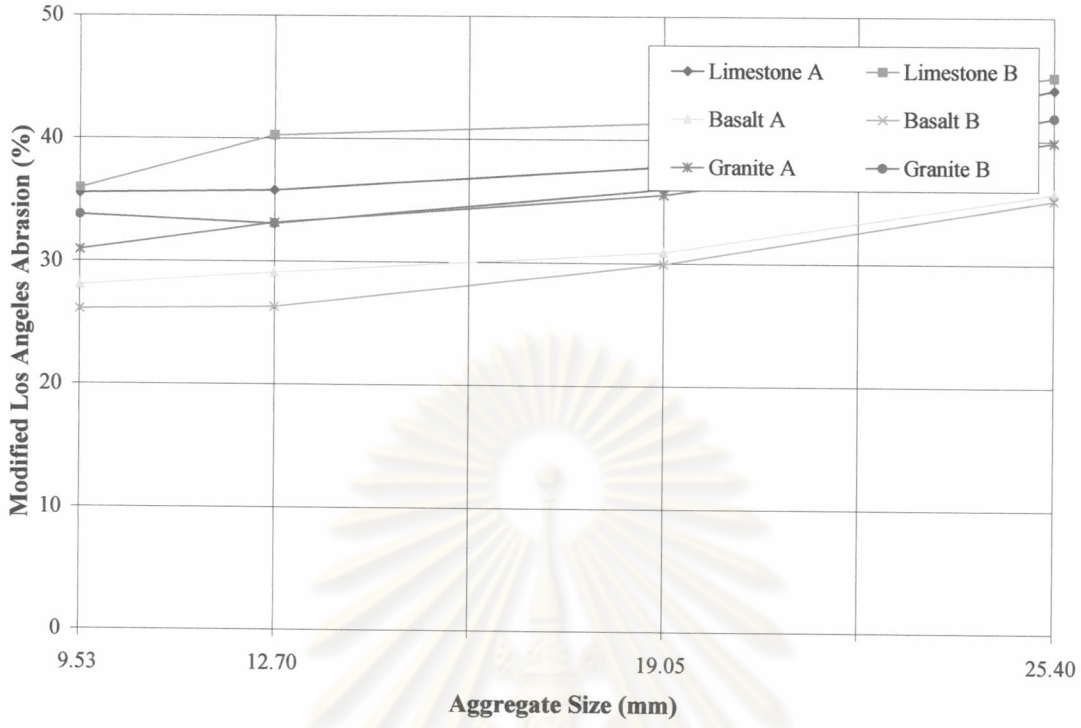


*Fig. 5.11 Modified Los Angeles abrasion of coarse aggregates with various sizes*

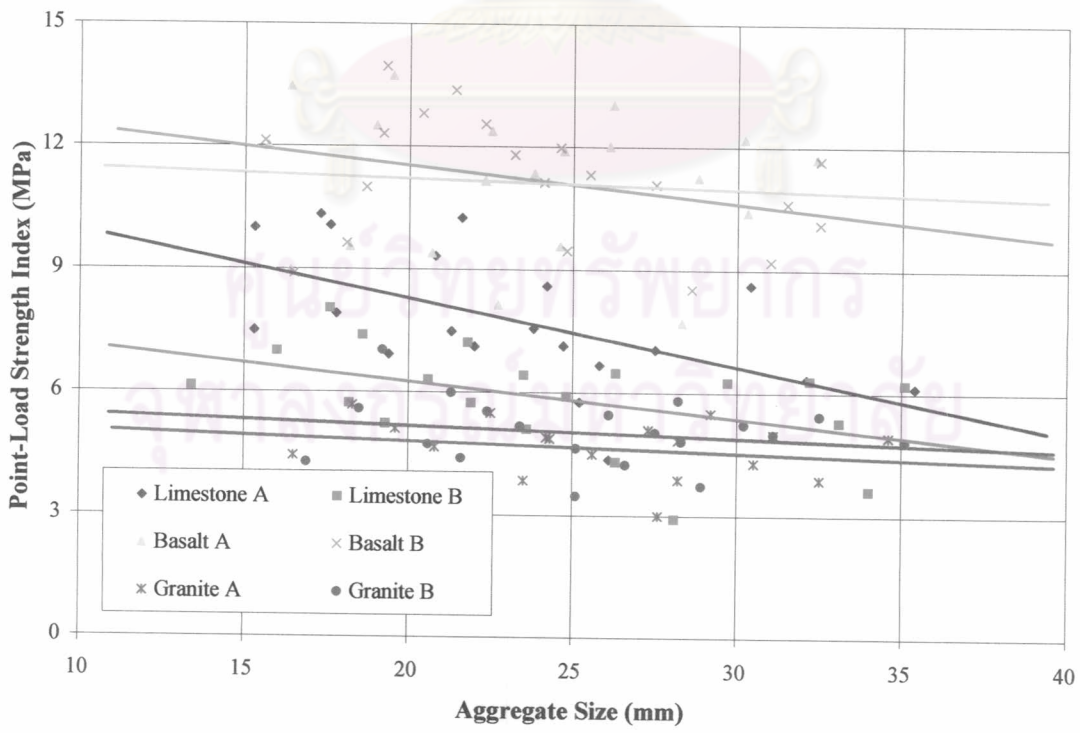


*Fig. 5.12 Point-load strength index of coarse aggregates with various sizes*

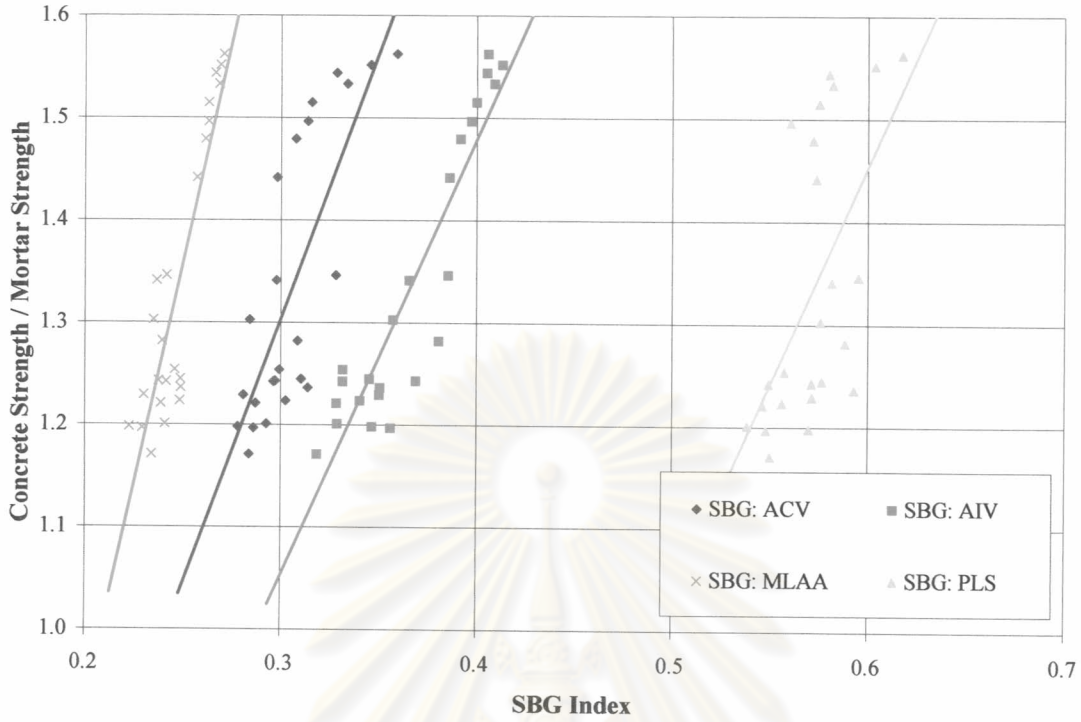


*Fig. 5.13 Ratio of concrete to mortar strength against SBG indices of various coarse aggregates*

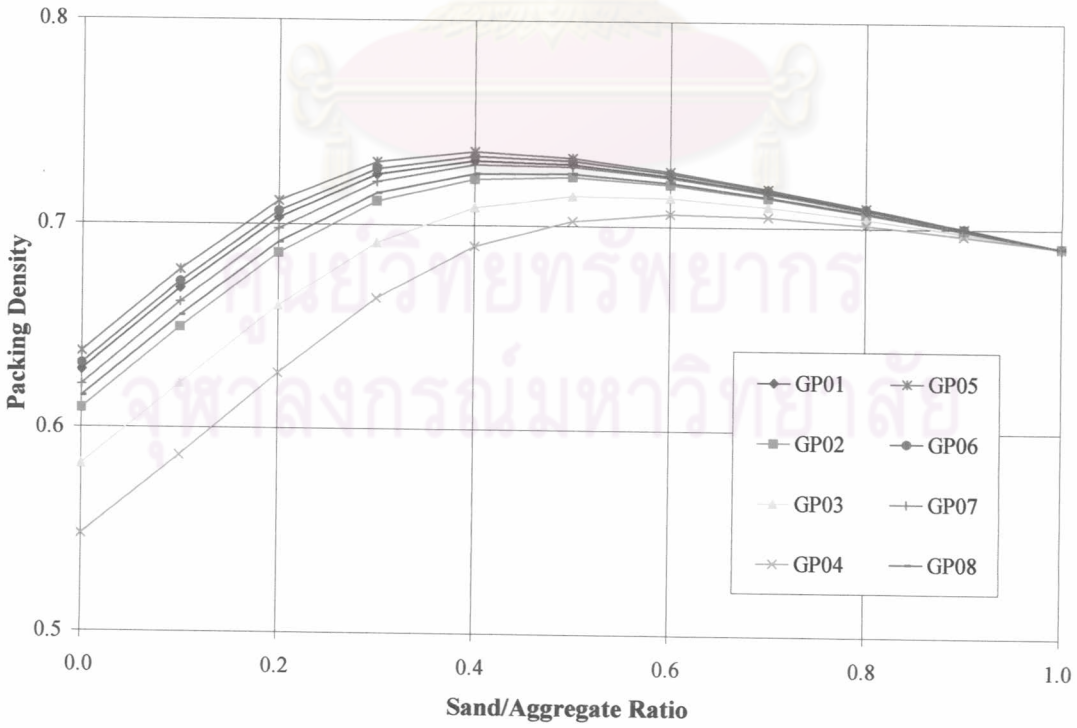


*Fig. 5.14 Packing density against S/A ratio of aggregate mixtures with 3.04-FM fine aggregate*

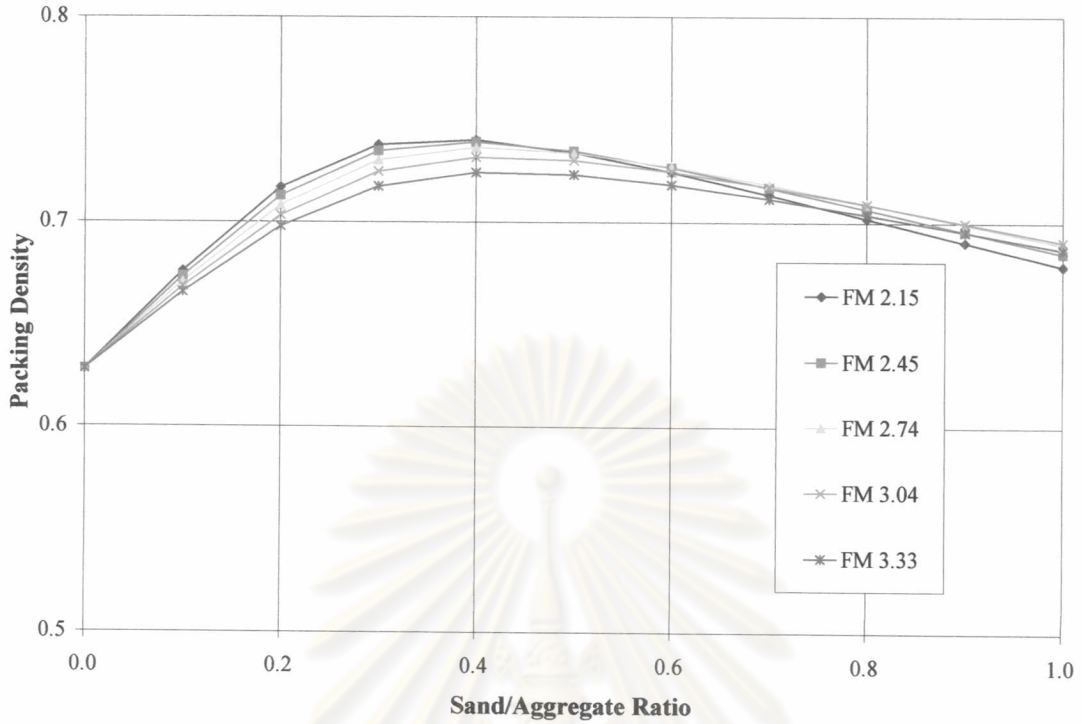


*Fig. 5.15 Packing density against S/A ratio of aggregate mixtures with GP01 coarse aggregate*

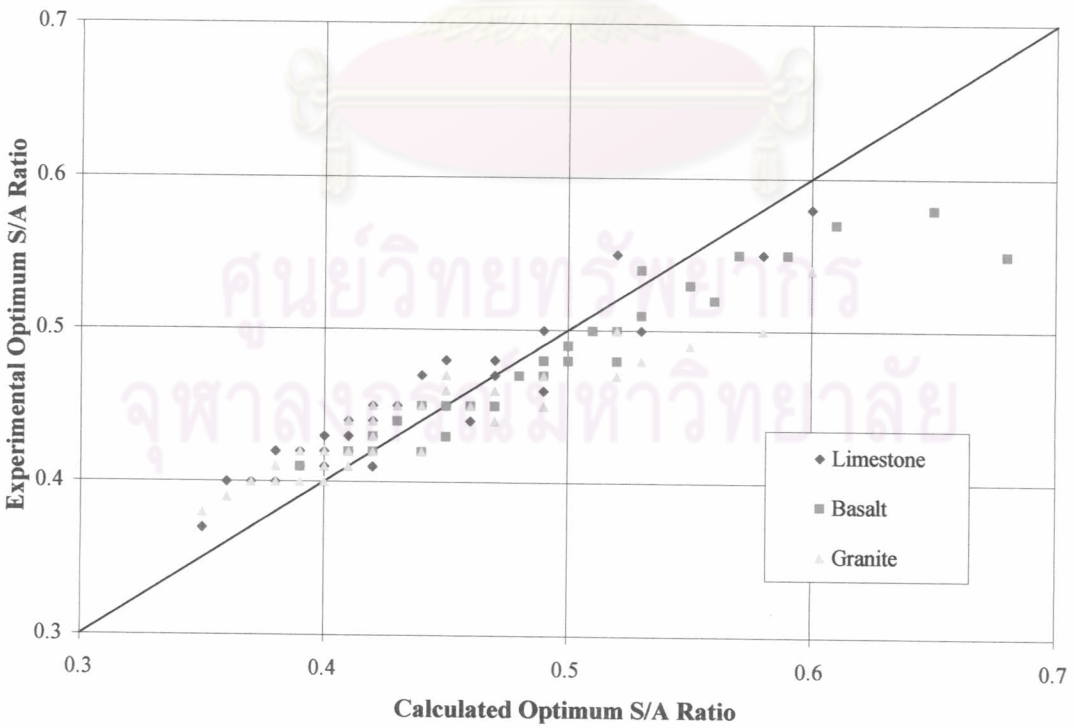


*Fig. 5.16 Comparison between optimum S/A ratio from experiment and calculation*

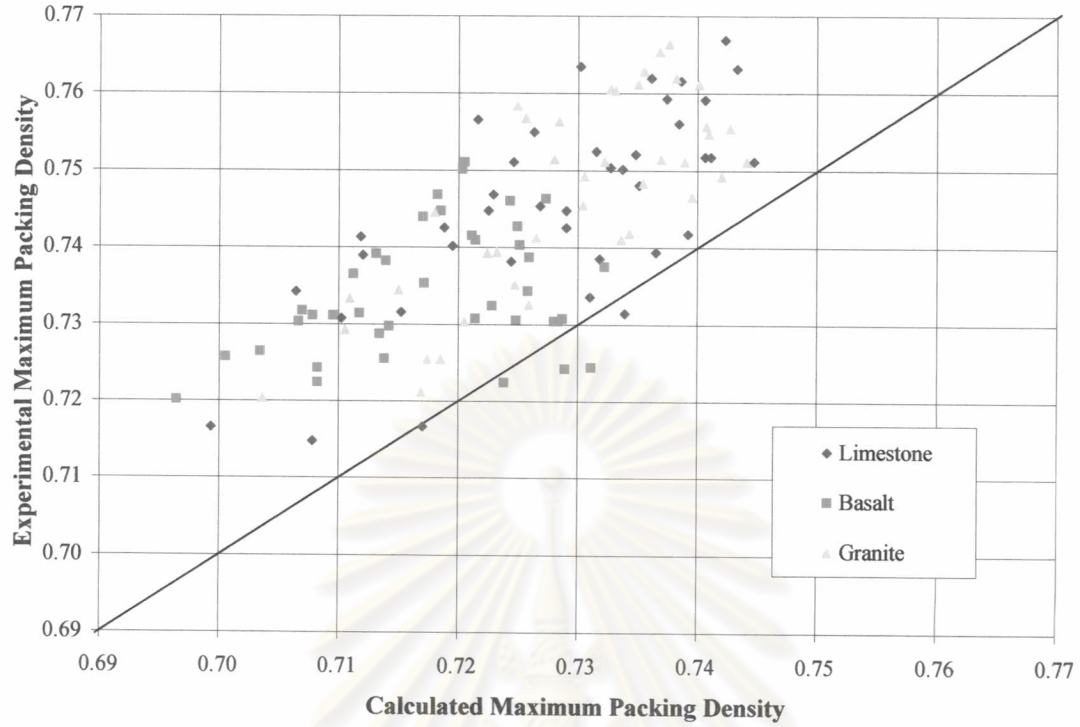


*Fig. 5.17 Comparison between maximum packing density from experiment and calculation*

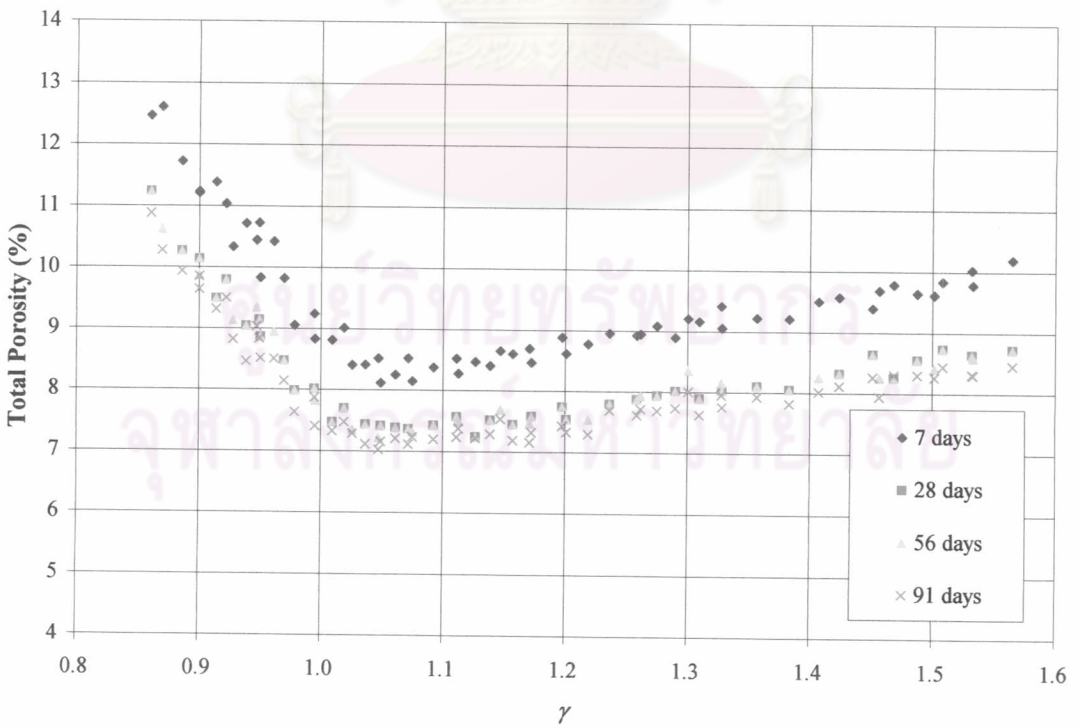


*Fig. 5.18 Total porosity of concrete with various ratio of paste to void content of dry and compacted aggregate*

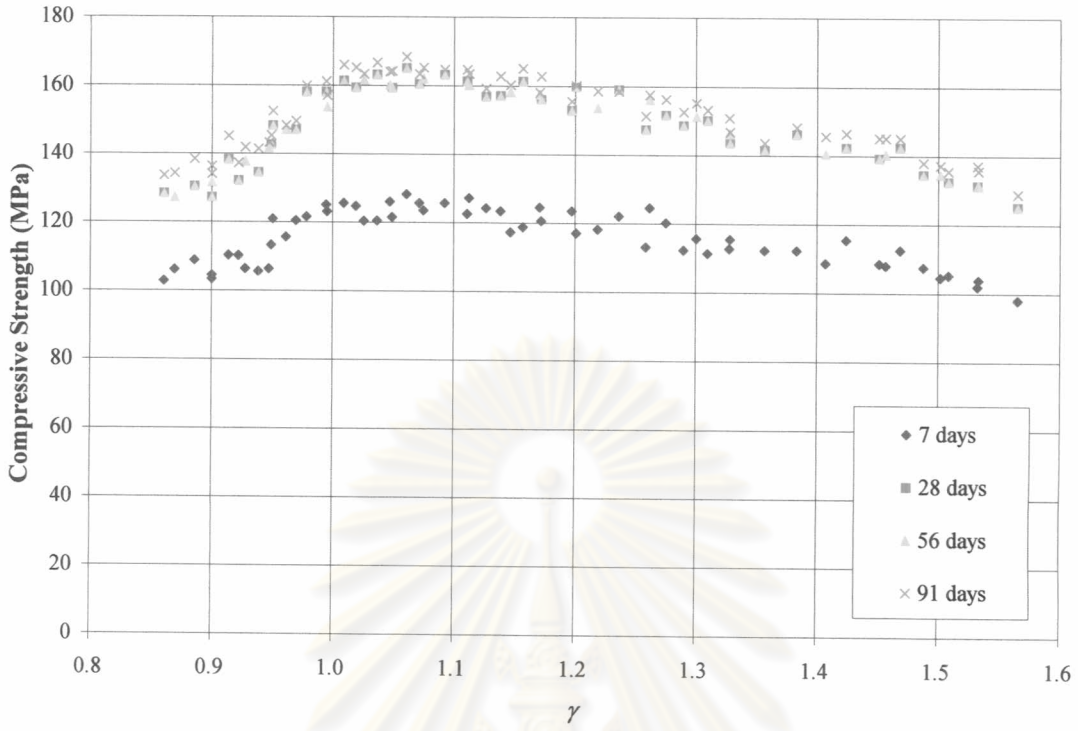


***Fig. 5.19*** *Compressive strength of concrete with various ratio of paste to void content of dry and compacted aggregate*

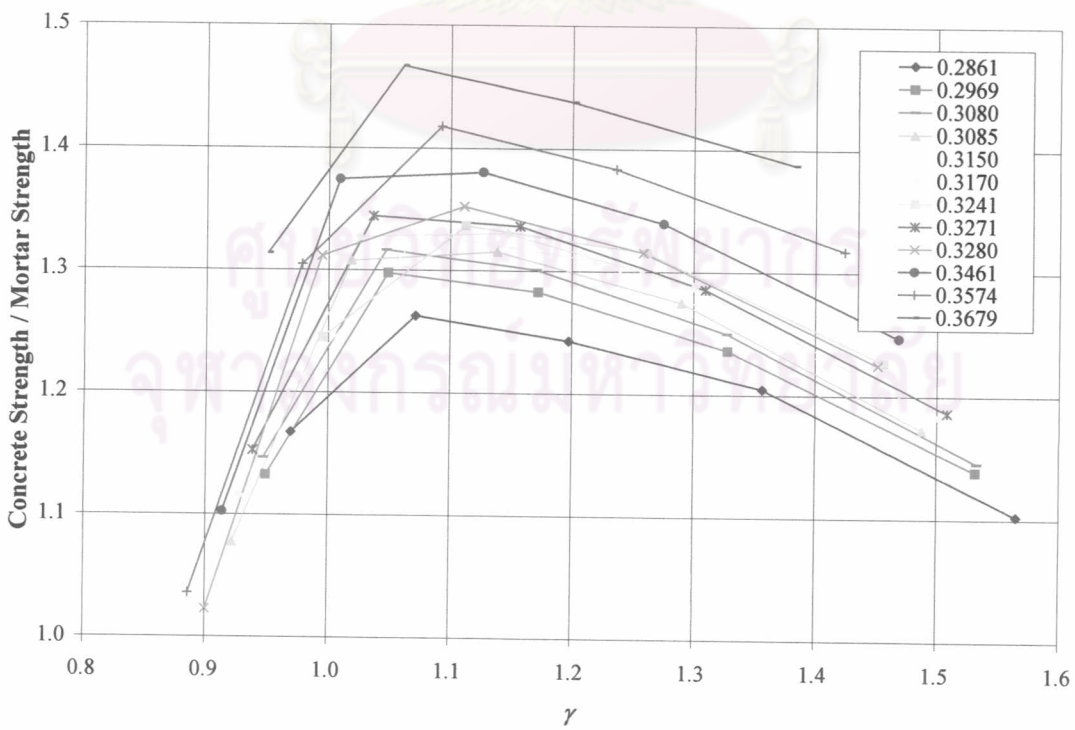


***Fig. 5.20*** *Concrete to mortar strength against γ of concrete with various SBG index*

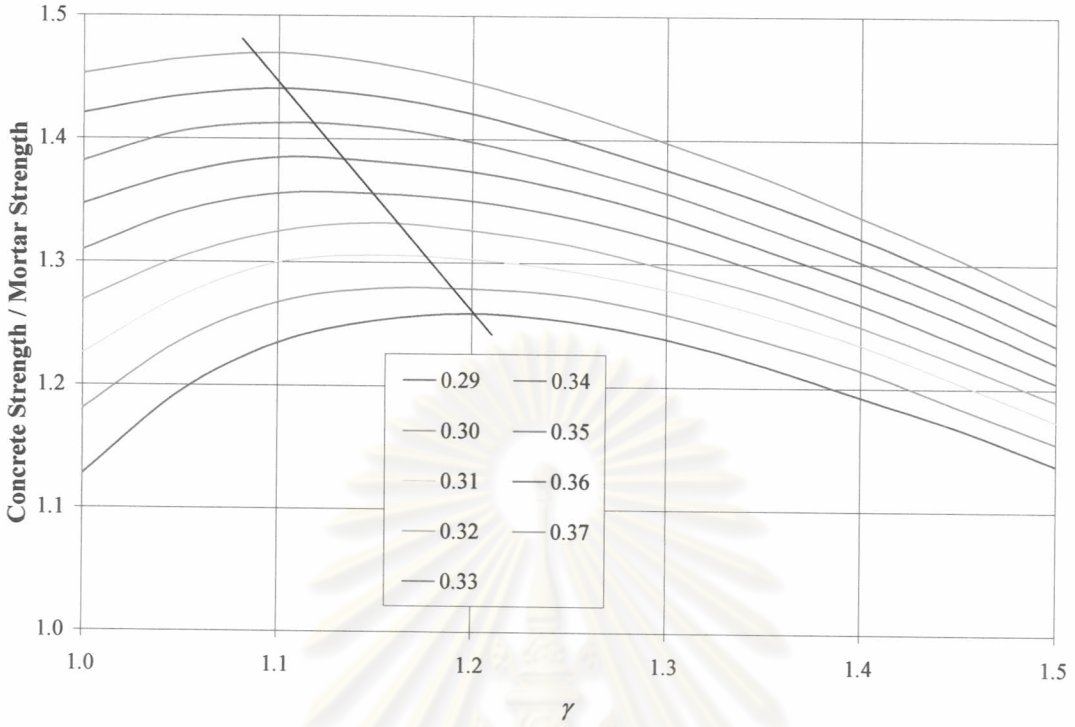


***Fig. 5.21*** *Interaction for concrete to mortar strength against SBG index and $\gamma$ of concrete*